LUND UNIVERSITY

Binding of moisture in fly ash blended Portland cement paste and mortar

Impact of replacement level and curing temperature

Linderoth, Oskar

2018

Document Version:
Publisher's PDF, also known as Version of record

[Link to publication](#)

Citation for published version (APA):
Linderoth, O. (2018). *Binding of moisture in fly ash blended Portland cement paste and mortar: Impact of replacement level and curing temperature*. [Licentiate Thesis, Division of Building Materials]. Lund University.

Total number of authors:
1

Binding of moisture in fly ash blended Portland cement paste and mortar

Oskar Linderoth
Building Materials | Faculty of Engineering | Lund University

Binding of moisture in fly ash blended Portland cement paste and mortar

Impact of replacement level and curing temperature

Oskar Linderoth

LUND
UNIVERSITY

Table of Contents

List of publications

I.   Examining hydration kinetics obtained from different mixing procedures using isothermal calorimetry

O. Linderoth, L. Wadsö
Proceedings: International RILEM Conference on Materials, Systems and Structures in Civil Engineering.
22-24 August 2016, Technical University of Denmark, Lyngby, Denmark.

II.   A strategy to determine the binder content of cementitious samples using hydrochloric acid and ICP-OES analysis

O. Linderoth, P. Johansson
Manuscript

III.   Binding of moisture in fly ash blended cement pastes and mortars

O. Linderoth, P. Johansson
Manuscript

Nomenclature

Symbols

α	Degree of hydration	%
B	Binder content	g
c	Cement content	g
H	Chemically bound water per gram of binder	%
W_e	Physically bound water	g
W_n	Chemically bound water	g

Abbreviations

A	Al_2O_3
AFm	Monosulphate
AFt	Ettringite
C	CaO
C/S	Calcium to silicon ratio
C_3A	Calcium aluminate hydrate
C_4AF	Calcium aluminate ferrite
CH	Calcium hydroxide
C-S-H	Calcium silicate hydrate
C_2S	Dicalcium silicate
C_3S	Tricalcium silicate
D_{50}	Median particle size
DVS	Dynamic vapour sorption
F	Fe_2O_3
FA	Fly ash
ICP-OES	Inductively coupled plasma optical emission spectroscopy
IGP	Intraglobule pores
ITZ	Interfacial transition zone

LGP	Large gel pores
MIP	Mercury intrusion porosimetry
OPC	Ordinary Portland cement
RH	Relative humidity
S	SiO_2
SCM	Supplementary cementitious material
SEM	Scanning electron microscopy
SGP	Small gel pores
TGA	Thermogravimetric analysis
w/b	Water-to-binder ratio
w/c	Water-to-cement ratio
XRD-Rietveld	X-ray diffraction with Rietveld analysis
XRF	X-ray fluorescence

Acknowledgement

I would like to thank my supervisor, Dr. Peter Johansson, as well as my co-supervisors Prof. Lars Wadsö and Dr. Katja Fridh; without their support and advice, this thesis would not have been possible.

I would also like to acknowledge my colleagues, present and past, at the Division of Building Materials. Thank you for letting me have my own spot in the lunch-room.

To my ever-supportive family and friends, thank you.

Lund, April 2018

Oskar Linderoth

Abstract

Water is a vital part of cement-based materials, but it is also closely related to many deterioration processes in and in contact with cementitious structures. The initial water, added in the mixing of e.g. concrete, is either bound chemically in the hydrates that result from hydration (the reaction between cement and water), or physically in the porous structure of the hardened cement paste. An understanding of how moisture is distributed in the material is important in order to predict the drying of concrete structures. The prediction is also crucial in order to assess the risk of moisture dependent deterioration of building materials applied to the concrete surface, e.g. flooring materials.

The frequent use of cement-based materials, along with the increasing awareness of climate change has put pressure on the cement and concrete industry to produce more sustainable products. In an effort to reduce CO_2 emissions, cements containing increasing amounts of supplementary cementitious materials – partially replacing the Portland cement– are produced. However, knowledge about the structural development and binding of moisture in concrete based on cements blended with supplementary cementitious materials is still limited.

In this thesis, the microstructural build-up and binding of moisture was studied in cement paste and mortar containing Portland cement or Portland cement where 10–60 wt% had been replaced by fly ash. The mortar samples were picked out of a larger volume of material, meaning that their binder content varied. To allow comparisons between the mortar samples, a novel strategy to determine the binder content was developed, resulting in **Paper II**.

A number of experimental methods were used to follow the chemical and physical binding of moisture in the material, from the first days up to six months of hydration. TGA and XRD-Rietveld analysis were used to study the chemically bound water. The results show that the total amount of chemically bound water decreases with increasing fly ash replacement, and that even small amounts of fly ash cannot fully make up for the loss of Portland cement within the first six months.

To measure the physically bound water, desorption isotherms were determined at different times after mixing. The isotherms show that less water is bound within most of the hygroscopic range (0–98% relative humidity) when 35 wt% of the Portland cement is replaced by fly ash after 28 days of hydration. At the same time, the desorption isotherms of Portland cement and Portland cement with 15 wt% fly ash replacement are quite similar.

The most apparent change in the isotherms between 28 days and six months is that the slope of the isotherms decrease in the high-relative-humidity-range (80–95%), for the tested binders, most likely because coarse pores are refined by the formation of additional hydrates. Additionally, the vertical order of the isotherms changes, and at six months, both of the fly ash blended isotherms are positioned above the OPC. This is in broad agreement with previous studies, stating that the total porosity is higher in blended cements compared to OPC, which may be explained by the fact that fly ash is less hydraulic and thus decreases the total degree of hydration. Additionally, previous

9

studies have found that the fly ash reaction does not increase the volume of solid material as much as that of Portland cement.

Mortar samples of both Portland cement and fly ash blended Portland cement, were hydrated at different curing temperatures (5, 20, 35 °C) during the first month. TGA measurements show that the amount of chemically bound water increases with temperature at early age, but that it is the opposite at later age, despite that all samples were moved to 20 °C after the first month of hydration. This temperature effect is not seen as clearly for chemically bound water in Portland cement with 35 wt% fly ash.

Desorption isotherms of mortar containing Portland cement and Portland cement with 35 wt% fly ash hydrated at different temperatures were determined at 28 days of hydration. The results show that, whereas the amount of chemically bound water was roughly the same in all samples according to the TGA, the porosity corresponding to the upper half of the isotherms increased with temperature. This effect of temperature is possibly the result of an apparent density increase with temperature, as reported in previous publications.

Sammanfattning

Vatten är en självklar del av cementbaserade material, men också nära kopplat till flera nedbrytningsprocesser i, och i kontakt med cementbundna konstruktioner. Det initiala vattnet, som adderas när materialet blandas, kommer antingen att bindas kemiskt i hydrat (genom hydratationen, cementets reaktion med vatten), eller fysikaliskt i porstrukturen hos den hårdnade cement pastan. Förståelsen för hur fukten är fördelad i materialet är viktig för att kunna prediktera uttorkningen av betongkonstruktioner. Predikteringen har avgörande betydelse också för att bedöma risken för fuktberoende nedbrytning av byggnadsmaterial som appliceras mot betongen, exempelvis golvbeläggningsmaterial.

Den stora användningen av cement baserade material, tillsammans med en ökad klimatmedvetenhet, sätter press på cement- och betongindustrin att producera mer hållbara material. För att minska CO_2-utsläppen produceras därför allt mer cement där delar av det traditionella Portlandcementet ersatts av mineraliska tillsatsmaterial, det vill säga blandcement. Men, kunskapen om strukturutvecklingen och fuktbindningen hos betong baserad på blandcement jämfört med den baserad på rent Portlandcement är fortfarande begränsad.

I denna avhandling studerades hur den mikrostrukturella uppbyggnaden och bindningen av fukt påverkas när delar av Portlandcementet ersätts med flygaska. Mätningar har gjorts på cementpasta och bruksprov, dels innehållande enbart Portlandcement som bindemedel och dels Portlandcement där 10–60 vikts-% ersatts med flygaska. Bruksproven plockas ut från en större volym material vilket betyder att andelen bindemedel i varje prov varierar. För att möjliggöra jämförelser mellan bruksproven behöver därför bindemedelsinnehållet bestämmas. Detta görs enligt en ny metod, vilken presenteras i **Paper II**.

Ett antal experimentella metoder användes för att studera den kemiska respektive fysikaliska bindningen av vatten hos prov av olika ålder, från de första dygnen upp till sex månaders hydratation. TGA och XRD-Rietveld användes för studera den kemiska bindningen av vatten. Resultaten visar att den totala mängden kemiskt bundet vatten minskar med flygaskeinblandning och också att en ökad inblandning ger en minskad mängd kemiskt bundet vatten. Eftersom provens högsta hydratationsålder var sex månader är det emellertid oklart om skillnaden i kemiskt bundet vatten kvarstår även vid högre åldrar.

För att studera den fysikaliska bindningen av vatten bestämdes desorptionsisotermer för bruken. Resultaten visar att en mindre mängd vatten bundits, fysikaliskt, i det hygroskopiska fuktområdet (0–98% relativ fuktighet) när 35 vikt-% av Portland cementet ersatts av flygaska efter 28 dygns härdning. Samtidigt är desorptionsisotermerna för rent Portlandcement respektive Portlandcement med 15 vikt-% flygaska ganska lika vid samma tidpunkt.

Den största förändringen av formen på desorptionsisotermerna mellan 28 dygn och sex månader syns på lutningen i det höga fuktområdet (80–95% relativ fuktighet), vilken minskar för samtliga bindemedelskombinationer. Det är troligt att förändringen av isotermernas lutning beror på att de

grova porerna förfinas när ytterligare reaktionsprodukter bildas och delvis fyller ut dessa. Dessutom ändras den vertikala ordningen av kurvorna, där nu isotermerna för de båda flygaskainblandade bruken ligger högre än det innehållande rent Portland cement. I en tidigare studie av cement med mineraliska tillsatsmaterial rapporteras att den totala porositeten alltid kommer vara högre än i Portlandcement eftersom tillsatsmaterialen är mindre hydrauliska och därför sänker den totala hydratationsgraden. Dessutom har tidigare studier funnit att det binds mindre mängd vatten per reaktionsprodukt i exempelvis flygaskareaktionen jämfört med vanligt Portlandcement.

Bruksprov härdades också vid olika temperaturer (5, 20, 35°C) under första månaden. TGA mätningar visar att mängden kemiskt bundet vatten är högst vid hög temperatur i tidig ålder, men att det är tvärtom efter 6 månader i Portlandcementproven, trots att alla prov flyttats till 20°C efter den första månaden. Motsvarande temperatureffekt sågs inte hos flygaskaproven.

Även desorptionsisotermer mättes för bruken som härdats vid olika temperaturer. Resultaten efter 28 dygns härdning visar att, även om mängden kemiskt bundet vatten, är ungefär detsamma, ökar den andel porer som motsvarar av den övre halvan av desorptionsisotermen med härdningstemperaturen. Denna temperatureffekt kan möjligen förklaras av att skrymdensiteten hos vissa hydrat ökar med temperaturen, vilket rapporterats i tidigare publikationer.

1. Introduction

1.1. Background

Cementitious materials, mainly concrete, are the most used construction materials in the world [1, 2]. More than 1 m^3 of concrete per person is produced annually, resulting in billions of tons of material [3]. Concrete consists of a hydraulic binder (most often OPC), water, and aggregate. Its good strength, durability, and raw materials readily available at a low cost are some of the reasons why concrete has become so popular.

Compared to many other construction materials, concrete has a low environmental impact [4], but because it is produced in such large volumes, its contribution to the worldwide CO_2 emissions is significant. It is estimated that cement and concrete production produce approximately 5–8% of the annual man-made CO_2-emissions [3], and that approximately 60% of these emissions result from calcination, the reaction in which limestone is heated to produce CaO, which is the main constituent in OPC. The other 40% originates from burning of fuels to heat the kilns [4].

The future demand for cement and concrete is expected to increase, not least in newly industrialized countries such as China and India. Along with the increasing awareness of climate change, this puts pressure on the cement industry to reduce its emissions and produce more sustainable materials. There was a similar pressure for change in the 1970s following the energy crisis, which ultimately led to a significant reduction in the kiln fuel consumption [5]. Today, most major cement producers have reduced their energy consumption by optimizing the production process and increasing the use of non-fossil fuels, making Portland cement clinker production among the most efficient industrial thermal processes in the world [4]. According to Gartner [5], any further significant improvements in energy efficiency in the near future are unlikely.

SCMs, such as slag, fly ash, and silica fume, are used to replace part of the OPC and reduce the environmental impact of cementitious materials. Most SCMs are by-products from other industries, showing more or less hydraulic properties. Because they do not require calcination, the replacement of OPC by SCMs results in a significant reduction in CO_2 emissions. Whereas SCMs seem to be the most promising solution to further reduce emissions, they also change the chemistry of the binder, resulting in nano- and microstructural changes that may alter important material properties. Although they are the topic of much research, knowledge about these changes is still limited [6, 7].

This thesis focuses on the microstructural development in fly ash blended Portland cement pastes and mortars, and how water is bound in such material. Water is often added to excess during mixing of cementitious material. Whereas part of the initial water (at normal w/c ratios) is chemically

bound in hydrated phases, part of the excess water is physically bound (or adsorbed) in the material's porous structure. Drying of part of the latter is often needed before a building is put to use, to avoid the degradation of moisture-sensitive materials, such as adhesives and wood.

The introduction of fly ash, having a different chemical composition and being less hydraulic than OPC, changes the rate of hydration as well as the amount and types of hydration products that form. Overall, this changes the pore structure and thereby the binding of moisture. In order to predict how the drying of concrete structures is affected by the use of fly ash blended OPC there is a need to further the understanding of the microstructural development, as well as the distribution of chemically and physically bound water in such systems. This thesis aims to further this understanding, combining knowledge from previous studies with comparative measurements of microstructure and moisture binding in OPC and fly ash blended OPC pastes and mortars.

1.2. Aim and research questions

The aim of this postgraduate study is to further the knowledge of how the presence of fly ash and the curing temperature affects hydration, the microstructural development and finally the binding of moisture in cement paste and mortar. To achieve this, the following research questions were formulated:

How does fly ash replacement affect the rate of hydration and the hydrate composition?

What is the effect of temperature on the fly ash reaction?

How do fly ash replacement and curing temperature affect the pore structure?

How is the amount of chemically bound water affected by fly ash?

How does fly ash replacement affect the sorption isotherm?

What are the effects of curing temperature on the sorption isotherm?

2. Materials and methods

2.1. Materials

The results presented in this thesis, including most of the results in the enclosed publications, have been measured on cement paste or mortar containing two different OPCs, or OPC with partial replacement by fly ash. For the mortars, a siliceous sand (EN 196-1) was used as the aggregate. The chemical compositions of the OPCs and the fly ash are given in Table 1, and the clinker compositions of the two OPCs are given in Table 2.

Table 1
Chemical compositions of OPC1, OPC2, and fly ash (FA), determined by XRF analysis.

	OPC1	OPC2	FA
CaO	62.8	63.4	4.0
SiO_2	19.4	21.4	51.1
Al_2O_2	4.4	3.4	25.6
Fe_2O_2	3.1	4.1	6.6
MgO	2.8	1.8	2.8
Na_2O	0.3	0.2	0.9
K_2O	1.1	0.6	2.7
SO_3	3.7	2.7	0.5
Blaine surface (m^2/kg)	536	343	
LOI*	2.6	2.4	4.6

Table 2
Clinker mineral composition of two OPCs, determined by XRD-Rietveld analysis.

	OPC1	OPC2
C_3S	64.4	64.1
C_2S	11.3	12.8
C_3A	4.6	2.1
C_4AF	8.8	13.6

All paste and mortar samples were mixed with a w/b ratio of 0.45. Sand was added such that a cement paste to aggregate ratio of 60 to 40 vol% was obtained for the mortars. Details on the mixing and curing of the mortars and cement pastes are given in **Paper III**. The experimental matrix is shown in Table 3.

	OPC	FA
OPC1	100	-
OPC2	100	-
XFA*	100-X	X

*) where X is the fly ash replacement and may vary between 10 and 60 wt%.

All fly ash blended samples contain OPC1.

2.2. Isothermal calorimetry

Isothermal calorimetry is the measurement of thermal power – heat production rate – under constant-temperature conditions. It is a general experimental method that may be used to study almost any process, as long as it generates heat. It has been used in countless studies of cementitious materials to follow the hydration process, not least to study the effect of SCMs [8-13]. The method was used in **Paper I** and **III**, where its principles are described in some detail. Additionally, examples of results are presented in Chapter 3 of this thesis.

2.2. TGA

TGA is a common method to determine the amount of chemically bound (or non-evaporable) water (H) in cement-based materials [9, 13-16]. The method may be used to determine both the total amount of H, and the amount of water bound in specific reaction products. The method utilizes the fact that different hydrates decompose within different temperature intervals. The method is used and thoroughly described in **Paper III**, but some examples of results are also presented and discussed in Section 4.2.

2.3. XRD-Rietveld analysis

XRD with Rietveld analysis is mainly used to determine the amount of anhydrous cement clinker minerals and crystalline reaction products in hydrated cement-based materials, such as to calculate the degree of hydration (α) of the cement. The method has been used in numerous publications, e.g. [14, 17-20], as well as in the enclosed **Paper III**.

In the present study, samples of approximately 3 grams were back-loaded and measured on a Bruker Endeavor 8 with Lynx Eye XE detector and automatic anti-scatter screen. The patterns were acquired over a 2θ range of 8–65°. A quantitative Rietveld analysis was done using Panalytical Highscore plus. The refinement was carried out by adopting the amount of Quartz in standard sand (EN 196-1) as an internal standard. The measured results are presented in Section 4.2.

2.4. DVS

DVS is used to measure sorption isotherms, showing the physically bound moisture content as a function of RH in equilibrium. Sorption isotherms may be measured in absorption or desorption, i.e. from a dry to a saturated state or vice versa. The method is described in further detail in **Paper III,** where several results are given. Additionally, some measured examples are presented and discussed in Section 4.3, all of which show the second desorption isotherms (i.e. the samples had been re-saturated from a dry state before the start of the measurements).

2.5. Arresting hydration

To arrest hydration (the reaction between cement and water), and to remove the evaporable water (bound in the porous structure), 5-mm-thick discs of mortar are placed in sealed plastic boxes with a controlled RH environment. The RH inside the boxes is maintained at 11% by circulating dry air from an air compressor. The RH was chosen to allow storage of the samples, while minimizing the risk of carbonation and removal of chemically bound water from the hydration products [21, 22]; 11% was thus defined as the dry state.

According to Powers and Brownyard [23], hydration slows down rapidly as the RH decreases from a saturated state, and it virtually ceases below 80%. The method was verified by the weighing of reference samples, as presented in Fig. 1.
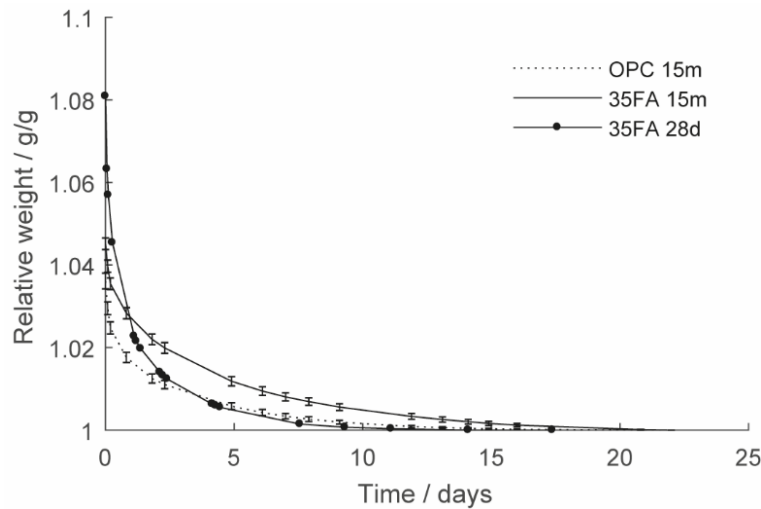

Figure 1
Drying of fresh OPC1 and 35FA mortar discs (5 mm), hydrated at 20°C for 28 days or 15 months. The curves obtained for the 15-month-old samples are the means of three observations.

All samples, including the reference samples, have been cured in sealed moulds, which means that no water, aside from the initial mixing water, has been added to the system; it is safe to assume that self-desiccation (chemical binding of water during hydration) has caused the RH to drop well below saturation. Thus, the samples may be partially dried already as they are placed in the boxes.

From the results it seems likely that most of the hydration ceases within the first day or two of hydration, even in the well-hydrated 15-month-old samples. However, reaching the dry state

17

(approximately 11% RH) takes a longer time. To be on the safe side, it was decided that for measurements requiring dry samples (e.g. TGA), the discs were to be stored under sealed conditions for no less than six weeks.

2.6. Binder content analysis

Most of the measurements presented in this thesis, as well as the enclosed papers, are carried out on mortar samples taken from a larger volume of material. Hence, to compare the results of different samples, there is a need to assess the binder content of each sample. This is done using the strategy presented in **Paper II**. The samples are dissolved in a specific volume of hydrochloric acid, determined by the sample mass. ICP-OES [24] is then used to determine the calcium concentration of the acid solution. Knowing the calcium fraction of the binder, it is then possible to calculate the binder content of the samples.

3. Cement-based material

This chapter gives an overview of the underlying reactions and mechanisms that give rise to hardened cement paste and its associated properties. The first section presents the chemical reactions that occur, and the phases that form, as Portland cement is mixed with water. The second section gives an overview of the hydration process. The third section is devoted to the hydration products, where special attention is given to the main hydration product, calcium silicate hydrate (C-S-H). The following section reviews some common SCMs, especially fly ash that was included in the cements used in **Paper II** and **III**.

Finally, a description of how hydration and the hydration products are related to the formation of a porous structure in cement-based material is presented. The most recognized structural models are presented and discussed. The pore structure reflects the material's potential to bind water physically and results from water binding chemically as hydrates are formed.

3.1. Hydration reactions

When water comes into contact with Portland cement, a series of reactions occur. These reactions are generally described by one term, hydration. Hydration is a complex process, as Portland cement consists of several clinker minerals, each reacting at a different rate, forming different hydrates. The four main clinker minerals are tricalcium silicate (C_3S), dicalcium silicate (C_2S), tricalcium aluminate (C_3A), and calcium aluminoferrite (C_4AF). Comprehensive reviews on cement hydration have been given by e.g. Taylor [25] and Odler in [26]. Additionally, several review articles on the mechanisms of cement hydration have been published in recent years, not only for OPC but also for blended cements, e.g. [7, 27, 28].

The typical OPC contains more than 50% of C_3S and lower amounts of C_2S, C_3A, and C_4AF. Calcium silicates are responsible for the formation of calcium hydroxide (CH) and C-S-H which make up the major part of hydrated cement paste. The hydrates form the cement paste that binds the aggregates together, giving the material its strength. The stoichiometric reactions of C_3S (1) and C_2S (2) are given in Eq. 2–3. As C-S-H does not have a univocal chemical composition, Eqs. 2–3 have intentionally been written with x, y and z rather than numerical coefficients.

$$C_3S + (3 - x + y)H \rightarrow C_x - S - H_y + (3 - x)CH \qquad (2)$$

$$C_2S + (2 - x + y)H \rightarrow C_x - S - H_y + (2 - x)CH \qquad (3)$$
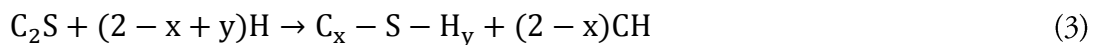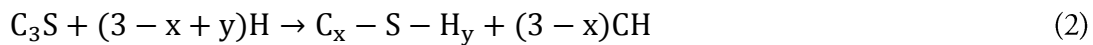
C_3A may react in different ways, depending on the surrounding circumstances. In contact with only water, the aluminate reaction is very rapid and may cause premature setting of the material. Premature setting limits workability and has a detrimental effect on important properties such as compressive strength. For this reason, sulphate, often in the form of gypsum, is added to cement. Gypsum slows down the aluminate reaction, giving it a rate pattern similar to that of C_3S [27], and

forming ettringite in the process (Eq. 4). When the system runs out of gypsum, the remaining aluminate reacts with ettringite to form monosulphate (Eq. 5). Finally, if all the ettringite is consumed, aluminate may react with CH from the silicate reactions to form a hydrogarnet phase, e.g. through Eq. 6. Hydrogarnets have a range of compositions of which C_4AH_{13}, is the most common.

$$C_3A + 3C\bar{S}H_2 + 26H \rightarrow C_6A\bar{S}_3H_{32} \tag{4}$$

$$2C_3A + C_6A\bar{S}_3H_{32} + 4H \rightarrow 3C_4A\bar{S}H_{12} \tag{5}$$

$$C_3A + CH + 12H \rightarrow C_4AH_{13} \tag{6}$$

The other aluminate phase, C_4AF, reacts similarly to C_3A, but at a lower rate, thereby forming ettringite, monosulphate and hydrogarnet, where some of the A is substituted for F. However, when containing F, the reaction products are no longer pure ettringite and monosulphate, despite the structural similarities. A strict cement chemist would thus call them AFt and AFm instead, where t and m represent the number of sulphate ions, three and one, respectively. In OPC, the C_3A and C_4AF are mixed, such that no F-free products exist. For stringency, the terms AFt and AFm are thus used for all of them throughout this thesis.

3.2. The hydration process

Hydration is a dissolution-precipitation process, i.e. the clinker minerals are transformed into solid hydrates through the passage of ions in solution [27]. As soon as cement grains come into contact with water, they start to dissolve, releasing heat and ions as chemical bonds in the clinker phases are broken. The mixing water then becomes a pore solution, containing a large number of different ions. The composition of the pore solution depends on the solubility of the clinker minerals. C_3A and gypsum are both very soluble and thus dissolve quickly. The main clinker mineral, C_3S, is also soluble, and contributes significantly to the early dissolution [29, 30]. The rapid early dissolution continues until the pore solution gets saturated or even supersaturated with ions, at which point hydrates starts to precipitate [31].

The heat production rate of an OPC mortar sample is shown in Fig. 2. The curve gives an overview of the hydration process, and shows the early hydration divided into five stages. The dissolution processes described thus far occur within the first hour, as the solution rapidly transitions from an unsaturated to a saturated state, marked as (1) in Fig. 2.
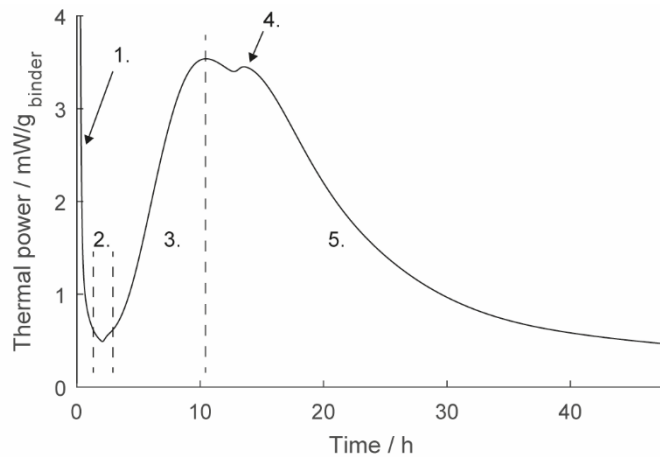
Figure 2
Heat production rate of a mortar sample containing OPC during the first 48 hours, measured by isothermal calorimetry (2.1).
Numbers 1-5 mark different stages of hydration, as explained in the text.

The saturation of the pore solution causes a slowdown in the dissolution, known as the induction period (2). The induction period is a period of low reaction rate, during which only minor amounts of e.g. ettringite and C-S-H precipitate [11]. Thomas et al. [32] state that this period is not a true induction period but that it occurs because the size and number of regions in which hydrates grow are still small. Occurring before the material has set, the induction period is of major importance e.g. in civil engineering, as it allows for concrete to be transported without loss of workability.

It is not entirely clear what influences the induction period and the same can be said about the onset of the acceleration period (3). According to Kumar et al. [29], the latter could be triggered by a sudden precipitation of CH. The following rapid acceleration is generally attributed to the growth of C-S-H [27, 28, 33], or more specifically C-S-H needles [34]. The C-S-H precipitation starts at the cement grains and aggregate surfaces and grows into the spaces between them to form a cement paste, along with e.g. CH. The production of hydrates results in a consumption of ions that allows for the continued dissolution of minerals, and thus the further occurrence of the reaction. The rapid formation of hydrates causes the material to set, drastically lowering the workability.

Simultaneous with the acceleration period, ions from C_3A and gypsum precipitate to form AFt phases. When all gypsum is depleted, the remaining C_3A dissolves rapidly, causing a second peak of heat release (4) [28]. The sulphate depletion peak occurs after the main peak, if the cement is properly balanced with respect to sulphate. Reports of a second and third peak related to C_3A and gypsum are found in [35], where the second peak is attributed to the transformation of AFt to more stable AFm phases.

Period (5) in Fig. 2 is known as the deceleration period. The mechanisms that cause the main hydration peak and thus the reaction to enter the deceleration period are not entirely clear. Previously, it has been attributed to the onset of a diffusion-controlled process; as the layer of hydrates grow thicker, it becomes harder for water to pass through, thus hindering further reaction. However, this theory is questioned in recent review articles [7, 28], as the measured results do not agree with the expectations of a diffusion-controlled reaction. Scrivener et al. [7] conclude that the main reaction peak seems to correspond to a dramatic slow-down in the growth of C-S-H needles, but the reasons for this are still not understood. Similar reasoning is found in e.g. [34], where it is

21

suggested that changes in the growth mechanisms of C-S-H could cause the deceleration. Dittrich et al [11] have shown that the peak of the main reaction coincides with the slowdown in C-S-H formation. Additionally, Berodier [36] found that C-S-H was homogenously distributed on all particle surfaces. Had diffusion been rate-limiting, aggregate surfaces close to cement grains would have had more hydration products, but this was not observed. Figure 3 shows the heat production rate of the two OPCs presented in Table 1.
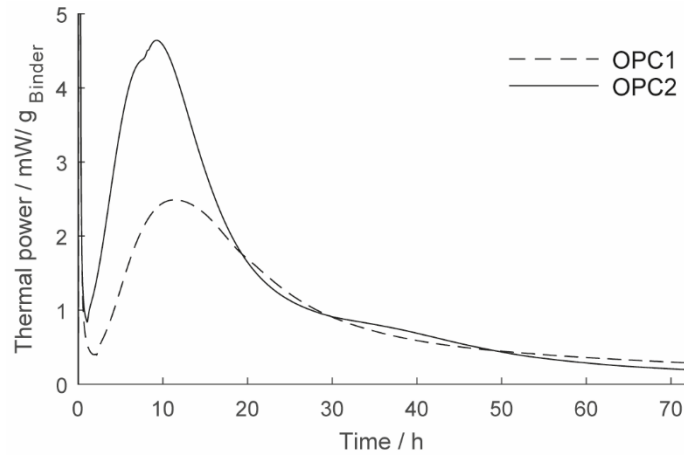

Figure 3
Heat production rate of two different OPC pastes during the first 72 hours, measured by isothermal calorimetry.

The clinker composition and fineness vary between the two OPCs (Table 1), which thus result in very different rates of reaction. Important early properties such as compressive strength may thus differ, depending on the type of OPC, and even more so when an OPC is blended with SCMs, as described in Section 3.4.

Although the rate of reaction slows down significantly after the first days of hydration, it does not stop. Instead of diffusion, a lack of space for precipitation of hydrates is suggested as the rate-controlling factor that causes the reaction to slow down [7]. However, unless the material is dried, the cementitious structure and properties continues to develop for months, even years after mixing. In a recent publication by Olsson et al. [37], DVS measurements were performed on mortars hydrated for four years. Their results show that further development of the pore structure is still apparent even after several years. This is also observed by further increases in strength.

The effects of mixing intensity – speed, duration, and presence of aggregates – were investigated and discussed in **Paper I**. Similar, but more extensive studies have been published by Juilland et al. [30] as well as Han and Ferron [38]. By increasing the mixing intensity, the initial dissolution is enhanced, which shortens the induction period and increases the slope and peak of the acceleration period. Juilland et al. [30] attributes the enhanced dissolution to a more efficient transport of ions away from the dissolving grain surfaces. Consequently, this leads to an increased formation of C-S-H nuclei that has an accelerating effect on the precipitation rate during the acceleration period. It is clear that the effect of mixing intensity should not be overlooked, as it may have an effect on both the short- and long-term properties of the material.

Aside from mixing intensity and the binder composition, the curing temperature may affect the hydration process, the distribution of hydrates, and thereto following properties such as strength and durability. Like increased mixing intensity, elevated temperature seems to enhance the

dissolution and e.g. shorten the induction period [39]. A shortening of the induction period could be caused by a lower level of supersaturation, as kinetic restraints are more easily overcome with increased temperature [31]. Figure 4 shows the heat production rate of OPC and OPC blended with 35% fly ash (class F, see Fig. 9) cured at different temperatures.
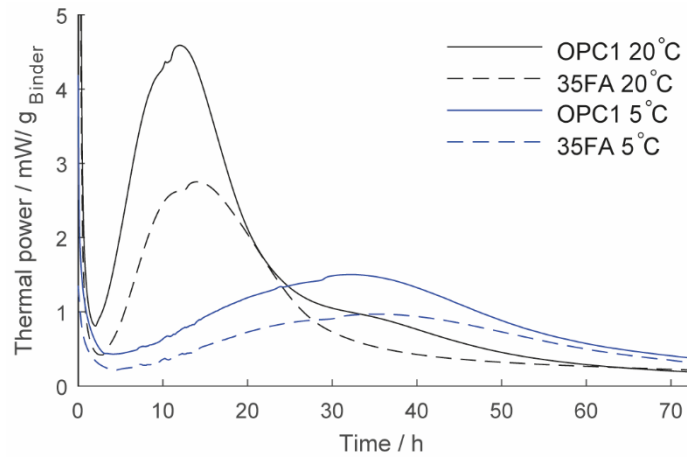

Figure 4
Heat production rate of cement pastes containing OPC1 or OPC1 blended with 35% fly ash hydrated at either 5 or 20 °C, measured by isothermal calorimetry.

As seen in Fig. 4, lowering the curing temperature severely retards the early rate of reaction. The effects of binder composition and curing temperature on hydration products and the resulting pore structure are described later (see Section 3.3 and 3.5), as well as in Chapter 4 and **Paper III,** where they are related to binding of moisture in the material.

Clearly, the mechanisms behind the early hydration process are a complex combination of multiple factors, e.g. the pore solution chemistry, particle surfaces, and their characteristics. Any further investigation of the early hydration mechanisms goes beyond the scope of this thesis. Instead the reader is referred to any of the extensive review articles written on this topic in recent years [7, 27, 28]. However, the effects of SCMs on early hydration are described in Section 3.4.

3.3. Hydration products

Hydration products form as ions from the dissolving clinker mineral precipitates. Together, the hydrates constitute a material called hydrated cement paste. The cement paste functions as the binder that holds the aggregates together, and thus the cement paste is responsible for most of the engineering properties of mortar and concrete. Thanks to the extensive laboratory studies by Powers and Brownyard [23], the properties of hardened Portland cement paste are well documented. Their work was recently revisited in two publications by Brouwers [40, 41].

As stated earlier, the seminal experimental studies by Powers and Brownyard [23] lay the foundation for our knowledge about hardened cement paste and its properties. However, understanding of the individual hydrates, i.e. the building blocks of the cement paste, their growth mechanisms and microstructural properties are far from complete, and still topics of much discussion [7, 27, 28].

The first subsection is focused on C-S-H, as it is the major hydrate phase, occupying almost 50% of the total paste volume. Consequently, it is most important for the microstructural development and thus the binding of moisture, both of which are properties within the scope of this thesis. The second subsection briefly presents the other major hydration products.

3.3.1. C-S-H

C-S-H is not only the most abundant hydration product, it is also responsible for many important properties of cement paste. Although it is not a very strong or stable phase, C-S-H forms a continuous gel that binds the cement and aggregate grains together, giving the final material its strength. Other hydration products, e.g. CH, form strong individual solid crystals but do not contribute much to the total strength.

As the main hydrate, C-S-H is also responsible for a majority of the chemical binding of moisture and thus to the formation of a porous structure. Additionally, C-S-H has a large intrinsic porosity, consisting of fine gel pores that contribute significantly to the physical binding of moisture. The importance of C-S-H for the structural development, and related properties is further discussed in Section 3.5 about pore structure as well as in Chapter 4 on moisture binding. This section focuses mainly on the formation and microstructural properties of C-S-H.

C-S-H is a complex phase that, despite thorough investigations [42-45], is still not fully understood. The main reasons for this are its varying structure and stoichiometry. Taylor [25] described the formation of two different types of C-S-H: outer (OP) and inner product (IP). In their recent review article Scrivener et al. [7], used the same nomenclature. Similar to OP and IP, Tennis and Jennings [46] also defined two types of C-S-H: low (LD) and high density (HD). In this thesis, the former nomenclature (OP/IP) is used. The two types are morphologically different, meaning their shape and microscopic structures are not the same, yet their chemical compositions are similar. Figure 5 shows schematic illustrations of OP and IP C-S-H growth.
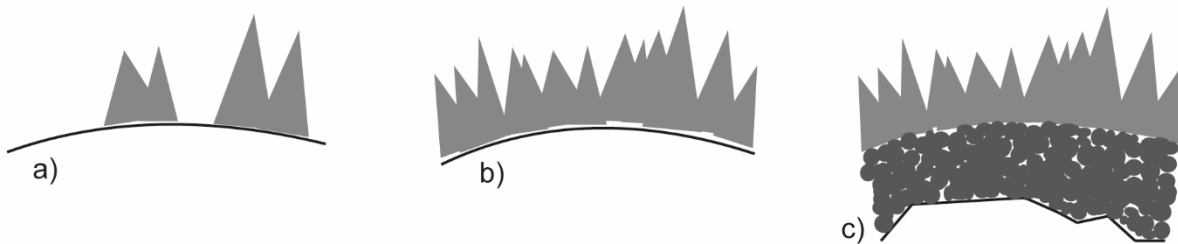

Figure 5
Growth of C-S-H: a) OP C-S-H precipitation on grain surfaces during the first hours, b) Needles cover the whole surface, conciding with the main peak of hydration, and c) Growth of IP C-S-H in the spaces between the dissolving grain and OP C-S-H. Adapted from [47].

Scrivener et al. [7] emphasize a C-S-H growth mechanism whereby OP C-S-H precipitates on the grain surfaces during the first hours after mixing (Fig. 5 a). The OP is described as loosely packed needles that shoot form the grain surfaces to occupy space that was previously filled with water [7, 34, 47]. The rapid formation of OP during the acceleration period causes setting and formation of a pore structure as the initial water phase is divided into capillary pores by the growing paste, as illustrated in Fig. 6.
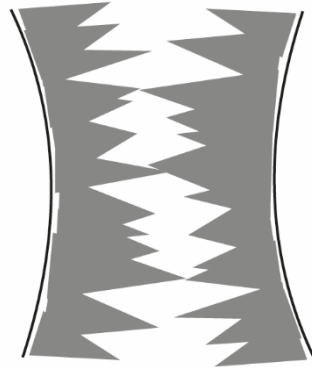
Figure 6
Schematic illustration showing the early formation of pores as C-S-H needles from two grain surfaces meet.

The growth of OP continues until the surfaces are covered with hydrates (Fig. 5 b), which coincides with the peak of the acceleration period (3) shown in Fig. 2. Beyond this time, a denser IP forms in the space between the dissolving cement grain and the OP (Fig. 5 c). C-S-H also forms in the remaining outer spaces. Although initially different, recent studies suggest that the C-S-H gel becomes more and more homogenous as hydration proceeds. Gallucci et al. [48] observed by SEM that in cement paste hydrated for one year, there were hardly any differences between the OP and IP. Muller et al. [49] found evidence that C-S-H densifies as hydration proceeds, as more dense hydration products form. Several models have been suggested to describe the microstructural build-up of C-S-H, e.g. [23, 43, 44, 50].

The growth and structure of C-S-H have proven very sensitive to changes in the surrounding conditions, e.g. temperature, relative humidity and composition of the reacting phases [6, 48, 51-55]. In the 1940s, Powers and Brownyard [23] stated that gels prepared at low temperatures were structurally different from those prepared at high temperature. Recently, Gallucci et al [48] showed that the apparent density of C-S-H increases by as much as 25% as the temperature rises from 5 to 60 °C, and similar results are also reported in [56, 57]. Densification of the C-S-H results in a more heterogeneous distribution of hydrates and increases the number of coarse pores as the hydration products occupy less space.

As stated above, studies have shown that C-S-H densifies continuously as hydration proceeds [49, 58]. According to Tomas and Jennings [52] the densification is slow under normal conditions but may be significantly accelerated by elevated temperature and drying. Their findings agree with previous studies suggesting that coarse porosity is increased with increasing curing temperature, at least for OPCs [16, 19, 59]. Coarsening of the pore structure also explain the detrimental effect of elevated temperature on the final compressive strength of concrete containing OPC [16, 60]. Interestingly, this temperature effect is not reported for blended cements (see Section 3.4).

Alterations of C-S-H caused by drying have proven problematic, as many microstructural measurements require the sample to be dry. Consequently, there has been much discussion of the extent of structural alterations caused by drying, whether they are reversible, and below which RH they occur [21, 22, 53, 54, 61, 62]. To the author's knowledge, there is no consensus regarding C-S-H and drying. However, most studies agree that the choice of drying technique should be carefully considered depending on e.g. the property of interest. This is especially important if the delicate C-S-H microstructure is to be preserved. Previous investigations [63, 64] have shown this

by studying the impact of different drying techniques on microstructural measurements such as DVS and MIP.

Paper III includes microstructural measurements conducted on samples pre-conditioned by drying. Sealed box drying (Section 2.5) was used, e.g. for the samples in **Paper III,** as the microstructure was to be preserved while also allowing the samples to be stored for several months.

3.3.2. Other hydrates

CH is the second product that forms from the calcium silicate (C_3S, C_2S) reactions. It is a crystalline phase of plate-like crystals that come in a wide range of sizes, mainly depending on the available space. Provided enough space, the plates may be several microns in size. However, most of the CH forms as much smaller crystals intimately mixed with C-S-H gel. CH does not have much impact on engineering properties such as strength, but is important for concrete's durability. CH is the most soluble hydrate and a major source of alkalinity. Therefore, the leaching of CH may increase porosity and thus the risk of e.g. chemical attack. Additionally, CH is consumed by the reaction of certain SCMs (see Section 3.4). Loss of CH lowers the pH, which may increase the risk of reinforcement corrosion.

AFm and AFt phases form by the reaction of C_3A and C_4AF. Like CH they do not have any major impact on the strength, but may increase the risk of chemical attack. The two groups of phases have very different morphologies, AFm forms plate-like crystals similar to those of CH, whereas AFt forms distinct rods.

In **Paper III**, TGA measurements of the CH content in mortars, with varying binder compositions are presented, and in Section 4.2 such results are also presented for materials hydrated at different temperatures.

3.4. Supplementary cementitious material

SCMs are used to improve certain properties and to reduce the amount of clinker for environmental reasons. Despite what the name suggests, SCMs are often used as a partial replacement of OPC. Thus, unlike aggregate that does not contribute to the hydration reaction, a SCM should have some hydraulic properties. Taylor [25] stated that the ability of a substance to act as a hydraulic cement depends on two factors:

- It should react with water to a sufficient extent.

- Reacting with water, it must yield solid products of very low solubility and with a microstructure that gives rise to the requisite mechanical strength, volume stability, and other necessary properties.

Three materials that fulfil Taylor's criteria are blast furnace slag, fly ash and silica fume, and they are the most common SCMs featured in modern cements. All three are by-products from other industries: slag from steelworks, fly ash from coal-fired electric power plants and silica fume from the production of silicon and ferrosilicon metal. Although environmentally favourable in the sense

that they require no additional clinkering process, they all originate from CO_2-heavy industries. However, at present, none of this CO_2 is assigned to the cement manufacturers.

The use of SCMs in cement is well established in the European building industry, and in 2008, the average clinker content of European cements had been reduced to 80% [3]. However, knowledge about the fundamental effects of SCMs on the hydration process and products is still insufficient (Lothenbach et al. [6]). It is clear that SCMs influence the rate of reaction as well as the number and type of hydrates that form. Therefore, they affect the structure of cement paste and thus important engineering properties such as durability and strength.

Irrespective of the type of SCM, the rate of reaction in blended cements is lower than in OPC equivalents. This is reflected by a lower heat production rate and a longer induction period before the reaction accelerates [10, 13]. With increasing SCM replacement, the OPC reaction is diluted, which prolongs the induction period, and delays the onset of acceleration. Typically, the SCM reaction only starts after a few days of hydration, depending on the replacement level, type of SCM, and curing conditions. However, before reacting, they may function as fillers, providing additional nucleation points for the OPC hydrates to precipitate. This so-called filler effect has been shown to accelerate the OPC reaction while also creating a more homogenous distribution of hydrates [65, 66]. Additionally, the efficient w/c ratio is increased in the presence of SCMs, which promotes the OPC reaction, as more water and space is available for the OPC hydrates. However, despite any accelerating effects on the OPC, even modest replacement levels of fly ash result in a lower early rate of reaction, as shown in Fig. 7.
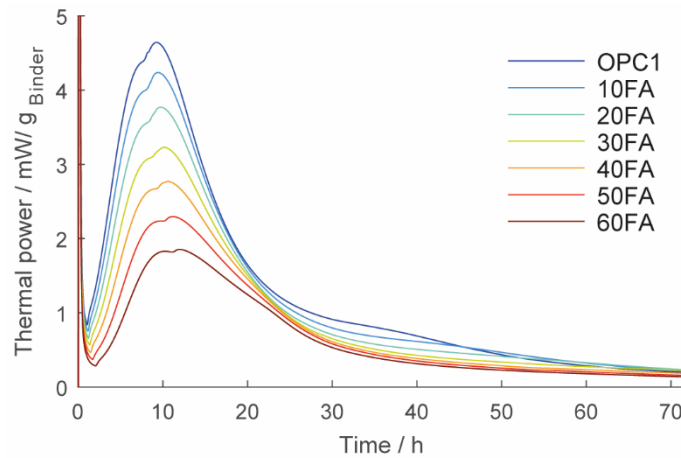

Figure 7
Heat production rate of cement pastes containing OPC1 and OPC1 with increasing fly ash (FA) replacement, measured by isothermal calorimetry.

The OPC reaction is increasingly diluted by fly ash replacement, as demonstrated by an extended induction period. The induction period is extended and deeper, as it takes a longer time to reach the critical ion concentrations that trigger acceleration. Very little fly ash reaction is noticed within the first three days. Figure 8 shows the results from Fig. 7 presented as per gram of OPC.
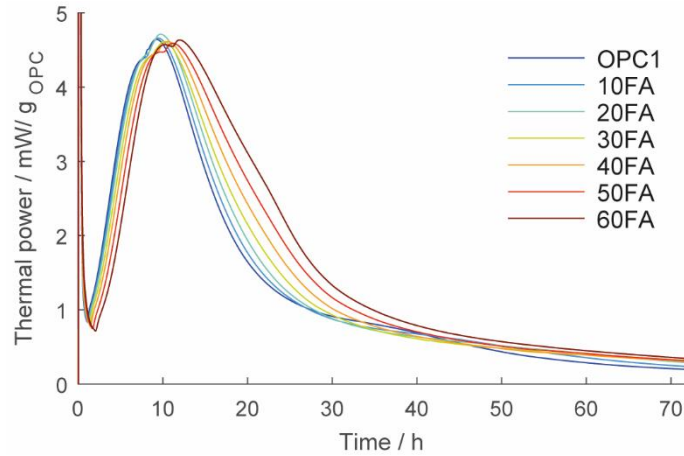
27

Figure 9
Heat production rate of cement pastes containing OPC1 and OPC1 with increasing fly ash (FA) replacement, measured by isothermal calorimetry.

The results presented per gram of OPC show the impact of fly ash on the OPC reaction and should thus reveal the filler effect. However, no filler effect is noticeable at any replacement level in Fig. 8, in contrast to the findings by e.g. Berodier and Scrivener [65]. A possible explanation for this is the fineness of the fly ash, indicated by the D_{50} value (median particle size). Berodier and Scrivener used an OPC with a D_{50} of 16 µm and a fly ash with 18 µm. The OPC in Fig. 8 is finer than theirs (11 µm) but the fly ash is coarser (30 µm). The addition of coarse fly ash may result in a surface reduction which reduces the nucleation points, having the opposite of a filler effect on the OPC reaction. From Fig. 8, it may be concluded that adding an SCM does not always result in an acceleration of the OPC reaction.

The main reason that SCMs react more slowly than OPC is revealed by their chemistry. Like Portland cement, most SCMs are composed of oxides of Ca, Si, and Al. Depending on their chemical composition, the SCMs are considered latent-hydraulic (blast furnace slag) or pozzolanic (fly ash and silica fume). This division reflects their hydraulic potential, i.e. the ability to react spontaneously with water. Figure 9 shows two ternary diagrams of CaO-SiO_2-Al_2O_3: A) containing OPC and some common SCMs, and B) the corresponding hydrates.

Figure 9
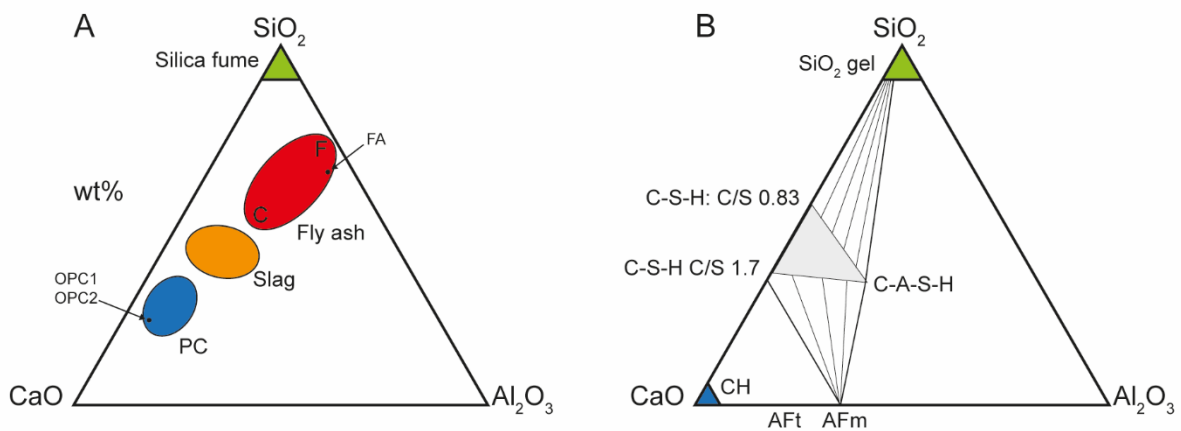Two CaO-Al_2O_3-SiO_2 ternary diagrams: A) OPC and some common SCMs, and B) the corresponding hydration products. The materials used in this thesis have been marked as OPC1, OPC2, and fly ash (FA). Adapted from [6].

As seen in Fig. 9, SCMs are Si- and Al-rich materials containing less Ca than Portland cement. The hydraulic potential decreases with decreasing Ca- content and a lack of Ca inhibits pozzolanic materials such as fly ash and silica fume from reacting directly with water. Instead, they are dependent on the formation of CH by the OPC reaction to produce C-S-H through Eq. (7). This reaction is known as the pozzolanic reaction and involves, apart from CH, SiO_2 from the SCM.

$$3CH + 2S \rightarrow 3C - 2S - 3H \tag{7}$$

The onset of the SCM reaction is thus dependent on the reactivity of the OPC (cf. Fig. 3, 3.3), but also on the pH of the pore solution. To trigger the dissolution of amorphous silicon in e.g. fly ash, the pH needs to be as high as 13, which is mainly governed by the number of alkali ions in the solution. Soluble alkali can be found both in OPC and in certain SCMs (see Tab. 1)

The choice of OPC should therefore depend on the type of SCM and the desired replacement level. Aside from the OPC, the hydraulic potential of each SCM governs its maximum practical replacement level [67]. Blast furnace slag is normally used at 20–70% replacement, whereas silica fume is limited to 5–12%. Fly ash is divided into class F and C (ASTM 618-15) with increasing CaO content (Fig. 9). The amount of fly ash in concrete may thus vary, from 5 to 65%, depending on the class. Fig. 10 shows the cumulative heat per gram of OPC for cement pastes containing OPC1 and OPC1 with increasing fly ash replacement. The differences between the OPC1 reference and the fly ash blended pastes likely arise from the reaction of fly ash, but also from an enhancement in the OPC reaction beyond the first days (as shown by the results in Fig. 19).
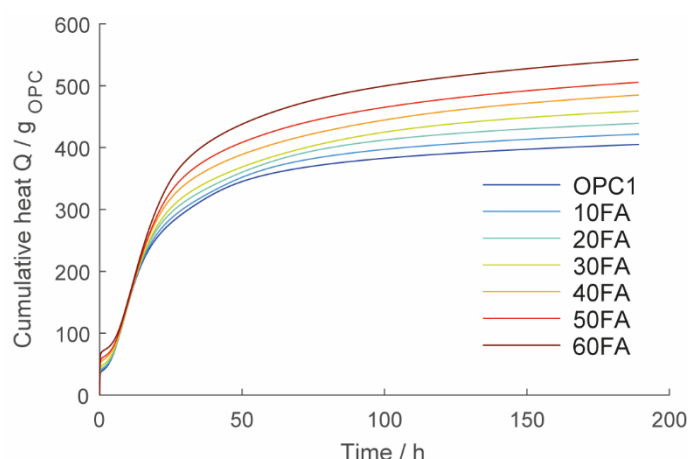

Figure 10
Cumulative heat release, per gram of OPC of cement pastes containing OPC1 and OPC1 with increasing fly ash (FA) replacement, measured by isothermal calorimetry.

Concerning the hydration products, the C/S-ratio of the C-S-H gel decreases in the presence of SCMs, as the C/S ratio of the system as a whole is lowered (Fig. 9). In e.g. fly ash blended systems, the uptake of Al in the C-S-H structure gives rise to C-A-S-H phases (Fig. 10), as well as additional AFm phases [6]. Changing the chemistry of the binder may also alter the growth conditions for the hydration products (e.g. ion concentrations), rate of precipitation, and the available space [27, 45, 68]. Significant differences in morphology have been reported between the C-S-H from OPC and blended cements. In OPC, it is described as 'fibrillar', whereas in blended cements, more 'foil-like', similar to OP and IP C-S-H (Fig. 5c).

Lothenbach et al. [6] used thermodynamic modelling to show that adding SCMs results in a lower volume of hydrates at complete hydration. Berodier and Scrivener [69] found that the reactions of slag and fly ash does not increase the volume of solids as much as that of the OPC, thus resulting in a higher total porosity. In contrast, there seems to be a general agreement that the long-term strength and transport properties of blended cements are superior to those of OPC [7]. A popular explanation for this is that SCMs refine the pore structure, i.e. result in a larger fraction of fine pores compared to the OPC. Possibly, this effect is enhanced by the different morphology of C-S-H formed by SCMs compared to that from OPC.

It should also be noted that, compared to OPC, blended cements react in a differently to temperature. As shown for fly ash and slag, the coarse porosity is reduced and the compressive strength increased by moderate elevations in the curing temperature [16, 20, 55]. Whereas the filler effect helps homogenize the distribution of hydrates early on – reducing the effect of elevated temperature on the OPC – the accelerated SCM reaction increases its space-filling capacity. In contrast, De Weerdt [16] showed that the reaction of fly ash is severely retarded at low temperature.

Furthermore, the amount of CH decreases in the presence of SCMs as it is consumed by the pozzolanic reaction. Additionally, less CH is produced as the amount of OPC is reduced. CH is a major source of alkalinity and lack of it may cause durability issues, such as chloride ingress and reinforcement corrosion. Further, in-depth discussions as to the effects of SCM on the hydration product are found in the review by Lothenbach et al. [6] and in the study by Escalante-Garcia and Sharp [59].

The use of fly ash blended cements is discussed in both **Paper II** and **III**. The effects of fly ash on the binding of moisture is discussed in **Paper III**. For these reasons fly ash is further discussed below.

The first major study on the use of fly ash in cement is likely that of Davis et al [70], published in 1937. The burning of coal for power generation began as early as the 1920s. However, before society became aware of the consequences of air pollution, the resulting particles were released to the atmosphere. This soon changed, and plants were fitted with equipment that prevented particle pollution, resulting in large amounts of fly ash residue [71]. Fly ash consists of spherical particles of different sizes, as shown in Fig. 11.
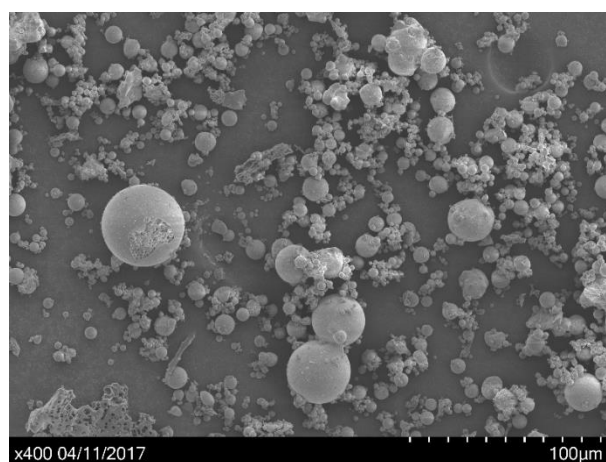

Figure 11
Clusters of fly ash particles captured by SEM.

30

The particles form while the fly ash in suspended in exhaust gases that are rapidly cooled. The rapid cooling means few minerals have time to crystallize. Instead, the fly ash particles consist of amorphous glassy phases. One exception is mullite, a crystalline phase consisting of aluminium-silicon. According to Neville [72], the glassy phase of fly ash is only dissolved once the pH exceeds 13.2. This explains why fly ash is dependent on the production of CH by the OPC reaction. CH is very alkaline and thus raises the pH of the pore solution. Figure 12 illustrates the build-up of a fly ash particle in cross-section.
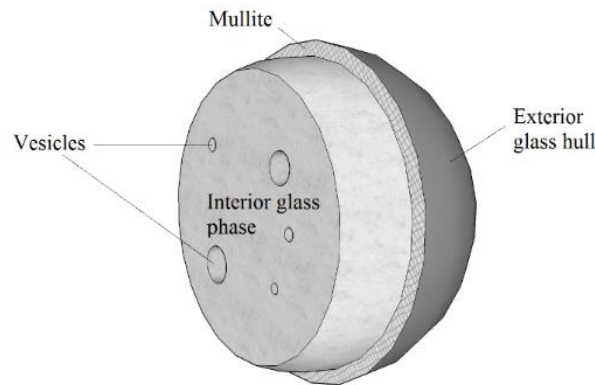

Figure 12
Schematic illustration of a fly ash particle in cross-section.

3.5. Pore structure

Several models have been suggested to describe the porous structure in cement-based materials. Two of the most recognized models are those of Powers and Brownyard [23] and Feldman and Sereda [50]. Their interpretations are schematically shown in Fig. 13.
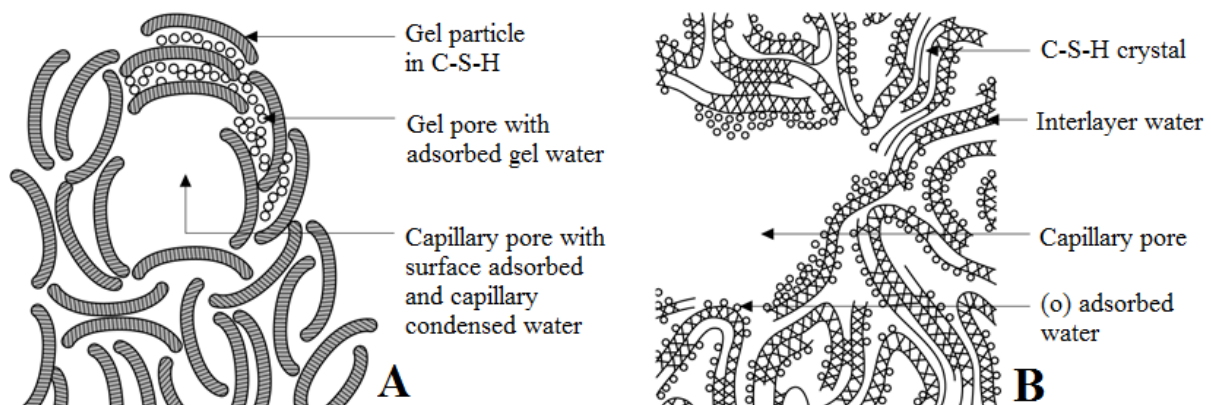

Figure 13
In A) Powers model of the microstructure, including C-S-H. B) The model by Feldman and Sereda. Translated and used with permission from [73].

As seen in Fig. 13, the models have much in common. Both describe C-S-H as having a layered structure; the main difference is found in the description of the fine cement gel structure. Powers and Brownyard describe this structure as consisting of small gel particles (without distinguishing between C-S-H and CH). Between the gel particles are fine gel pores, containing adsorbed water,

so-called gel water. Larger capillary pores form as spaces between the cement grains are encapsulated by the growing cement gel. The capillary pores are defined as spaces larger than approximately 2.7 nm in diameter, assuming cylindrical pores. Water in the capillaries is considered 'free', unbound water.

According to Feldman and Sereda, C-S-H consists of irregular arrays of single layers that come together randomly to form interlayer spaces. The interlayer water is only lost upon strong drying, starting at approximatley 30% RH, but most pronounced below 11% RH [21]. The process is reversible, and water may re-enter the interlayers upon re-saturation. Adsorbed water is found on the C-S-H surfaces but, in contrast to Powers and Brownyard, they do not distinguish any gel pores. Capillary pores are formed in spaces that are not filled with hydrates. Figure 14 illustrates the nanostructure of a single C-S-H layer, or sheet, where water is chemically bound.
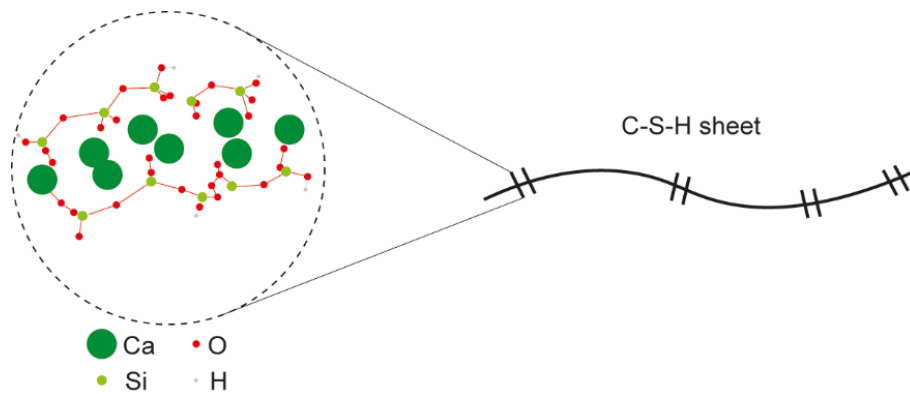

Figure 14
Schematic illustration of the nanostructure of a single C-S-H sheet, adapted from [74].

More recent models of C-S-H have been published by Jennings [43, 46]. The first model, CM-I, was published in 2000 and was later modified into CM-II in 2008. The CM-II model is schematically illustrated in Fig. 15.
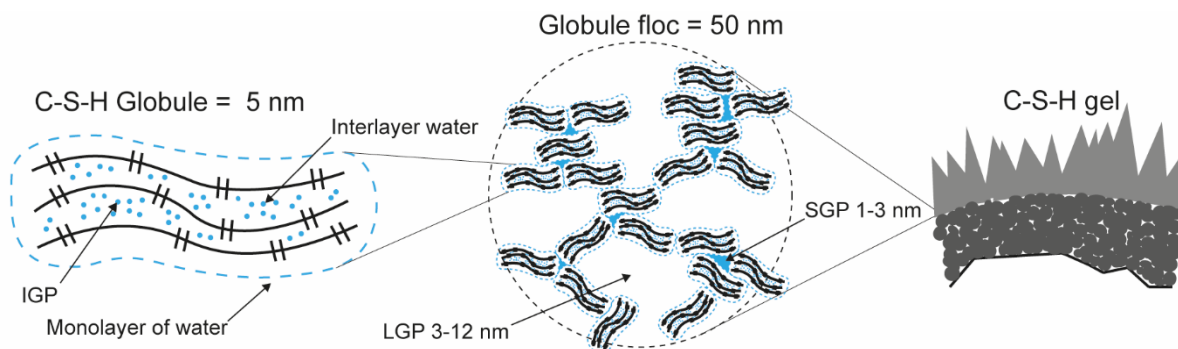
Figure 15
Schematic presentation of Jennings CM-II model for C-S-H. Adapted from [43].

C-S-H is described as consisting of small globules, approximately 5 nm in size. The globules have a layered structure with water bound in the interlayer spaces and IGP that are smaller than 1 nm. Additionally, a layer of adsorbed water is found on the globule surface in its saturated state. Multiple globules are packed together to form globule flocs. SGP forms between the globule particles and LGP between flocs of globule particles. Pores larger than 12 nm are referred to as capillary pores.

Powers and Brownyard [23] found that water may condense in pores above 45% RH, thereby marking the transition from gel to capillary porosity. Jennings defines gel pores as spaces emptied below 85% RH and divides them according to their size, as described above. It is the author's understanding that Jennings's division of gel and capillary porosity, in contrast to that of Powers', does not depend on the presence of capillary water but rather on how the pores were formed. By Jennings's definition, capillary pores are residuals of the initial water phase that decreases in volume as hydrates precipitate inside them. Gel pores are intrinsic to the C-S-H gel and thus increase in numbers as hydration proceeds. The CM-II model has been increasingly recognized in recent years. In a subsequent publication, Jennings [62] applied the model to sorption measurements in an effort to explain the structural changes caused by drying.

Modifications of the CM-II model could be justified based on recent findings by Muller et al. [49, 75], who found evidence of only two types of gel pores: interlayer water and SGP. Additionally, they found inter-hydrate spaces approximatley 10 nm in size, comparable to LGP in CM-II, but not intrinsic to the C-S-H. According to Scrivener et al. [7], inter-hydrates are probably related to spaces forming between needles of C-S-H.

Furthermore, Muller et al. [49] present evidence that the capillary porosity is refined to a threshold diameter, below which the number of gel pores no longer increases thus indicating a transition to the formation of denser C-S-H. The densification is explained by additional C-S-H sheets forming in the gel pore spaces, which lead to an increase in the overall C-S-H density. This increase could explain the decreasing differences between OP and IP C-S-H observed with time in [48].

Figure 16 schematically illustrates the coarse porosity (>10 nm) in the cementitious structure, including the inter-hydrate spaces defined by Muller et al. [49, 75].
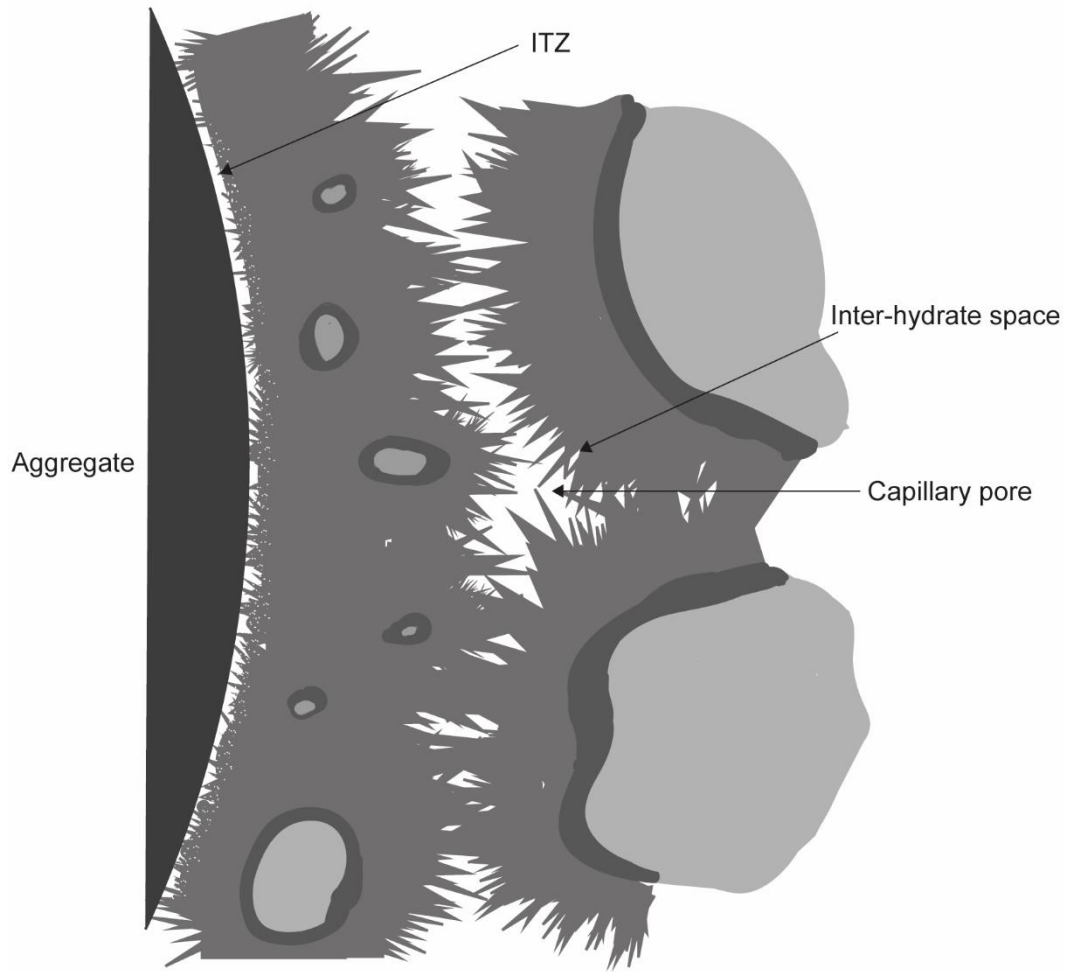
Figure 16
Schematic presentation of interhydrate spaces, capillary pores and the ITZ in a hardening concrete structure.

Inter-hydrate spaces and capillary pores contribute to the total porosity, and their presence thus effects the mechanical and moisture properties and potentially durability. Additionally, an ITZ forms between aggregate surfaces and the bulk cement paste, where the porosity is increased [76, 77]. The ITZ forms as the packing of the cement grains against the much larger aggregate results in a predominance of small cement particles close to the surface, as illustrated in Fig. 16. According to Scrivener et al. [77], the ITZ has an impact on certain mechanical properties, e.g. increasing the ductility. Furthermore, they found that the impact of the ITZ on transport properties, although significant, is counteracted and outweighed by other effects. Like the inter-hydrate and capillary pores, the ITZ decreases with increasing degree of hydration as hydrates fill the space. Zooming out even further reveals the coarsest pores, air voids, and micro-cracks, as shown in Fig. 17.
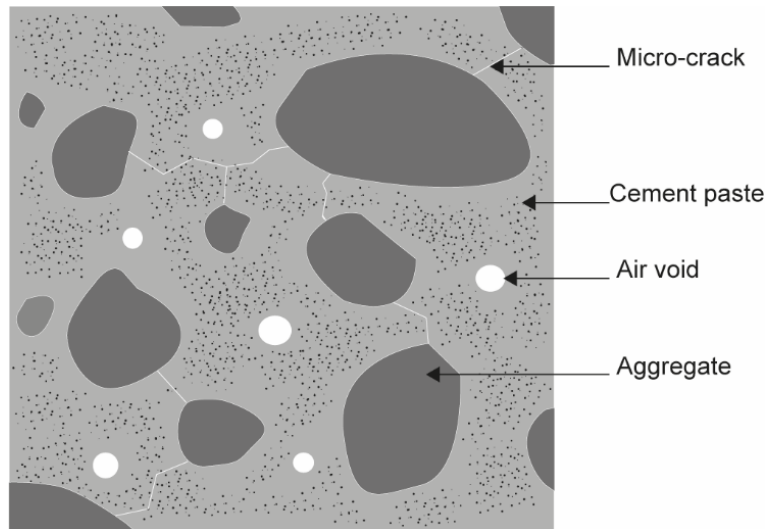
Figure 17
Schematic illustration of the concrete structure.

Air voids are e.g. important for the concretes resistance to freeze-thaw by buffering the volume expansion caused by ice formation. Micro-cracks may form 'naturally' as the concrete self-desiccates during hydration, resulting in chemical shrinkage. Additional cracks may also be caused by severe drying, which in turn could impact the transport properties. However, for the physical binding, or sorption, of moisture, air voids and micro-cracks are less important as their sizes cause them to empty at very high RH (>95%), close to saturation.

It is the author's understanding that most structural models agree upon the nature of the coarsest pore structure (>10 nm). The division of pores formulated by Jennings CM-II, with the addition of inter-hydrate spaces, has been used to analyse sorption measurements in Section 4.3, as well as in **Paper III**. Finally, it should be noted that all the mentioned models were developed for OPC, and thus any structural alterations caused by SCMs are not accounted for.

4. Moisture binding

This chapter gives an overview of how moisture is bound in the hardened structure of cement-based materials. Moisture may be bound chemically, in the hydration products, or physically in the porous structure of the material. These two types of bound moisture may also be termed non-evaporable and evaporable water. Additionally, close to saturation, bulk water (unbound) may exist in the structure, e.g. in air voids and micro-cracks.

4.1. Moisture in cement-based materials

Water is added to dry cement to initiate hydration. Part of the initial water is bound chemically in the hydration products, whereas excess water is bound physically in the material's porous structure. Partial drying of the physically bound water is often needed during construction, before a building is put to use, to avoid degradation of wood, polymer-based flooring materials, or adhesives in contact with or in close proximity to the concrete.

Aside from the initial water, the material may take up water from the surrounding environment. Water vapour in the air may diffuse into the material, and liquid water from e.g. rain, condensation, or ground water, may be absorbed. Naturally, water may also be lost, e.g. through evaporation, if the ambient water vapour content is lower than that of the material.

The following subsections discuss chemically and physically bound water and how they may be determined. Measured examples are presented and discussed, some of which are also found in **Paper III**.

4.2. Chemically bound water

The initial amount of water added to cement-based material is often in excess compared to what is theoretically required to reach a complete hydration. Traditionally, the complete hydration of 1 kg OPC is said to bind approximately 0.25 kg of water, chemically. This makes it possible to calculate the degree of hydration (α) using Eq. 7 [23].

$$\alpha = \frac{W_n}{c \cdot 0.25} \tag{7}$$

However, this value (0.25) is heavily dependent on the method applied to remove the evaporable water. Some methods, e.g. oven drying (105 °C), may destroy part of the ettringite and C-S-H, resulting in an underestimate of the chemically bound water content. True values for modern OPCs are likely higher, possibly in the range 0.3–0.35, as supported by findings in e.g. [16], the amount of H in Fig. 18, and in **Paper III**. It should also be noted that, for blended cements, the values are

generally lower than for OPC. To some extent, this is explained by the fact that SCMs are less hydraulic, but evidence also suggests that hydrates resulting from the SCM reactions bind less water than their OPC equivalents [6].

It should be noted that a theoretical maximum H is not the same as the minimum w/c ratio required to reach complete hydration, as the hydrates occupy a larger volume than the anhydrous cement and liquid water. Thus, the space available between the grains at the theoretical minimum w/c ratio will not be sufficient to allow complete hydration. Taking this into account, Powers and Brownyard [23] predicted a practical minimum w/c ratio of 0.42. While recapitulating their work, Brouwers [40, 41] found that for modern OPC, this value is approximately 0.39. However, even at these w/c ratios, reaching complete hydration takes a very long time, as the structure grows dense, slowing down the kinetics significantly. Despite never reaching complete hydration, lower w/c ratios than the practical minimum are often used in civil engineering applications, not the least to achieve rapid drying of the structure.

TGA (Section 2.2) is a common experimental method to measure both the total amount of chemically bound water as well as that bound in specific hydration products. Fig. 18 shows the total amount of H and the amount of CH in mortars made from OPC1 and 35FA.
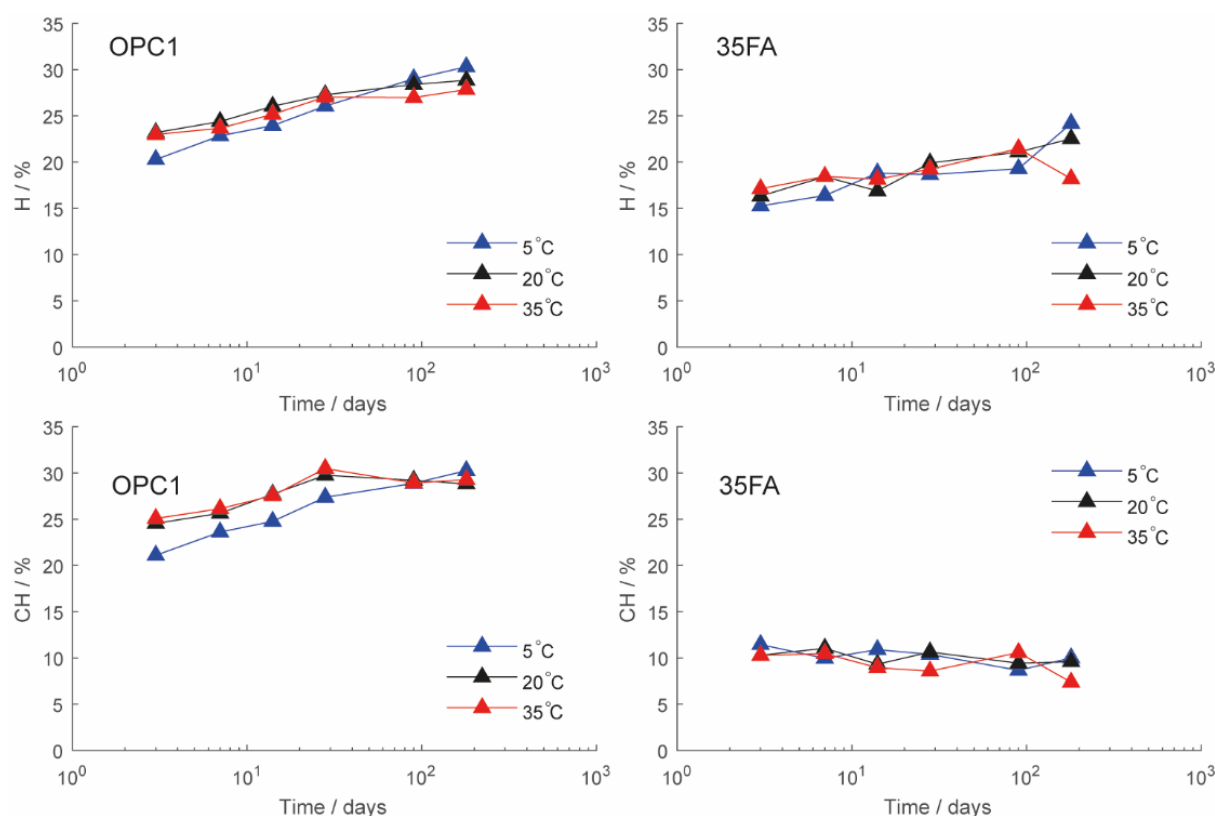
Figure 18
Amount of H (upper two) and CH (lower two), per gram of binder, in mortar containing OPC1 (left) and 35FA (right), measured by TGA. Beyond the first month, all samples were hydrated at 20°C.

The amount of H increases over time as hydration proceeds. Even if the curing temperature is the same (20°C) for all mortars beyond 28 days, there is a decrease in H with temperature in the OPC1 samples at six months of hydration. However, such a temperature effect is not observed in the 35FA

38

mortar. The results in Fig. 18 are in broad agreement with previous studies, e.g. De Weerdt et al. [14, 16] and Deschner et al. [57], who both used similar materials.

The results for CH in Fig. 18 reveal that a large part of the H-difference between OPC1 and 35FA can be explained by less CH in the latter. A majority of this CH-difference likely arises from the fact that there is 35% less CH-producing OPC present in the latter. However, part of the difference results from the pozzolanic reaction of fly ash that consumes CH to produce additional C-S-H.

XRD with Rietveld analysis (Section 2.3), is another method that may be used to study the chemical binding of moisture in cement-based materials. The method allows determination of the anhydrous clinker minerals, crystalline hydrates, as well as the amount of amorphous material. Provided the original clinker mineral distribution is known, it is possible to calculate the degrees of hydration (α) of each clinker mineral, as well as that of the OPC in total, using the XRD-Rietveld results. Figure 19 presents the development of α_{OPC} in OPC1 and 35FA mortars.
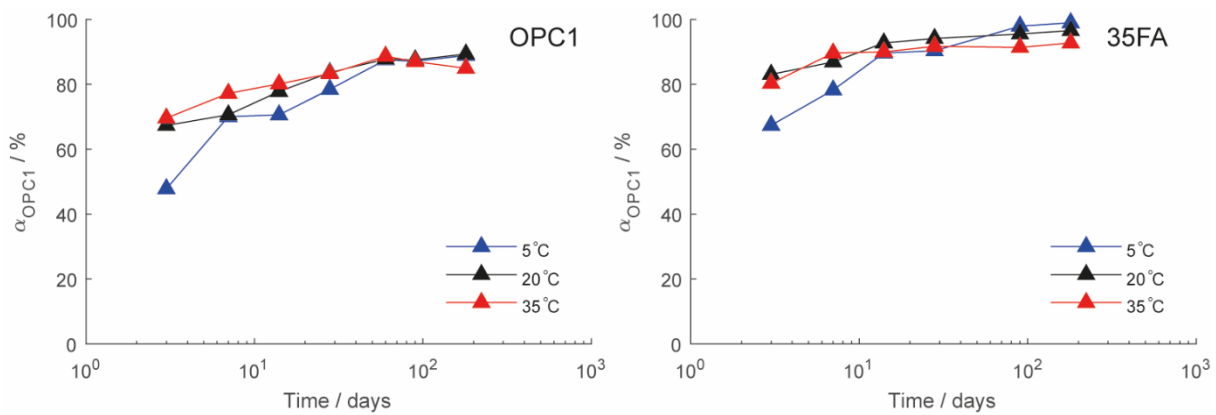

Figure 19
Degrees of hydration (α) in mortar containing OPC1 (left) and 35FA (right), determined by XRD-Rietveld analysis. The samples were all hydrated at 20 °C beyond the first month.

As seen in Fig. 19, the OPC reaction is enhanced in the presence of fly ash. However, from Fig. 9, it was concluded that the fly ash used in the present study does not give rise to any early filler effect (e.g. additional surfaces and nucleation points). Supported by recent publications [6, 7], it is the author's belief that the increase in α_{OPC} of the blended mortar is rather related to the available space. The pozzolanic nature of fly ash results in a slower reaction, fewer hydrates, and thus more space for the OPC hydrates to precipitate. In other words, the effective w/c ratio is increased in the 35FA mortar and the OPC is diluted.

However, had the w/b ratio been higher, it is likely that lack of space would not be an issue and that additional space provided by the fly ash would not give rise to any acceleration of the OPC. Correspondingly, lowering the w/b ratio will not necessarily enhance the effect of additional space, as the reduction of water also limits the maximum α.

Assuming the XRD-Rietveld results in Fig. 19 correspond with those of TGA in Fig. 18, it may be possible to calculate the maximum H in the OPC samples. For example, at six months, H is approximately 28.9% and α_{OPC} is 89.3% in the 20 °C sample; H_{max} would thus be approximately 32%. Fig. 20 presents H from TGA versus α_{OPC} from XRD-Rietveld.
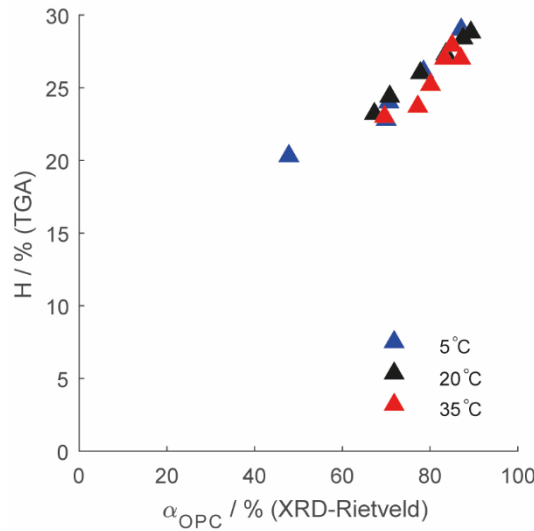
Figure 20
Comparison of α_{OPC} in the OPC1 samples from TGA and XRD-Rietveldt analysis, using the data presented for OPC1 in Figs. 18 and 19.

It is possible that a small part of the OPC have already reacted with moisture in the surrounding air before the addition of mixing water. For this reason, TGA analysis was performed on anhydrous OPC and the results were subtracted from the results of the hydrated materials. Yet, an extrapolation of the results in Fig. 20 does not end at the origin, but at a few percent on the y-axis. However, it is unlikely that the relationship between H and α_{OPC} is linear as the clinker minerals react at different rates, and bind different amounts of water. The first days of hydration are dominated by the reactions of C_3S and C_3A, whereas at later age the reactions of C_2S and C_4AF become all the more important (Fig. 21). This can possibly explain the results in Fig. 20.

As for the effect of temperature, the TGA (Fig. 18) and XRD-Rietveld (Fig. 19) results are broadly in agreement. In both systems, α_{OPC} reaches the highest values hydrating at low temperature. The fact that such a temperature effect is not seen, on the total amount of H, in the 35FA samples in Fig. 18 could indicate that the fly ash reaction is more sensitive to low temperatures than the OPC.

In Fig. 21, α_{OPC} has been divided into the contributions of three clinker minerals, and is presented for OPC1 and 35FA mortar hydrated at 20 °C.
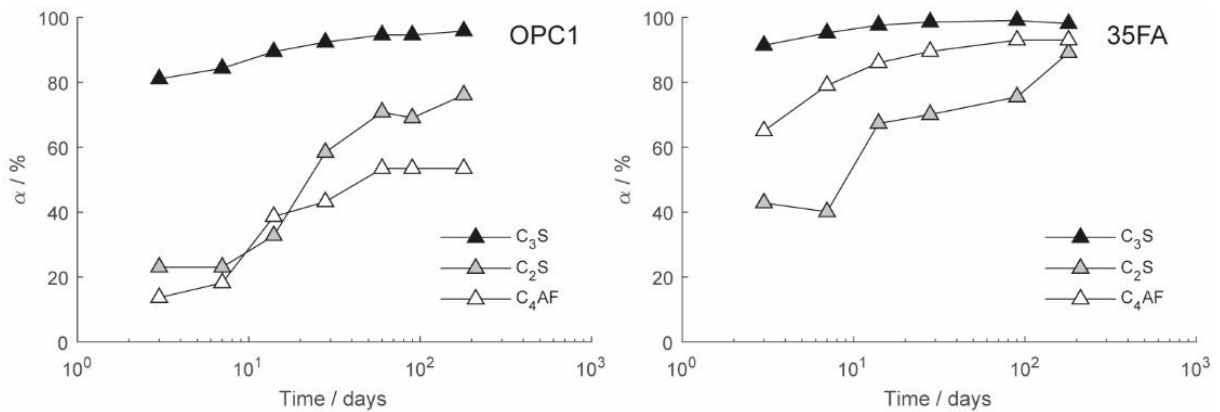

Figure 21
Degrees of hydration (α) of the individual clinker minerals in OPC1, from XRD-Rietveld analysis, for mortars hydrated at 20°C (also in **Paper III**).

40

Figure 21 shows that the reactions of C_2S and C_4AF are accelerated in the presence of fly ash. Both the results for α_{OPC} (Fig. 19) and those of the clinker minerals (Fig. 21), agree well with previous studies that used similar materials [16, 19, 20, 78]. As seen for OPC1 in Fig. 21, more than 80% of the C_3S has reacted in the first three days, whereas the C_2S and C_4AF reactions are much slower. Thus, increasing the available space will mainly enhance the C_2S and C_4AF reactions that would otherwise be affected by the lack of space. The fourth major clinker mineral, C_3A, has been purposely left out in Fig. 21 as its reaction is very rapid, reaching complete hydration within a week, irrespective of the binder composition.

In addition to the TGA and XRD-Rietveld results, SEM images were taken of the structure in the OPC1 mortars at six months of hydration, as shown in Fig. 22. The samples were hydrated at different temperatures during the first month.
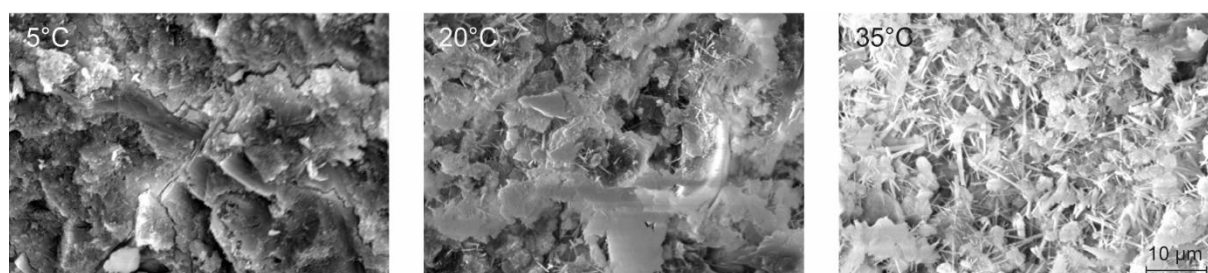

Figure 22
SEM images of six-month-old OPC1 mortar samples, hydrated at different temperatures (left to right: 5,20,35°C) for the first 28 days, and then at 20°C.

The images in Fig. 22 show an increase in coarse porosity with temperature, in agreement with previous studies [16, 19, 59]. To some extent, this is explained by the decrease in the amount of chemically bound water with temperature seen in Fig. 18 for OPC1. However, the increase in coarse pores may also be explained by an increase in the apparent C-S-H density with temperature, leading to more coarse pores, as shown for OPC in e.g. [48, 56] and for fly ash blended cements in [16]. In either case, it is clear that the first months curing temperature has a significant impact on the structure, including that at later ages.

4.3. Physically bound water

Water that is not bound chemically in the hydrates, or lost through evaporation, will be bound physically in the material's pore structure. The finer the pore, the stronger the bond between water and the pore surface. Upon drying from a saturated state, water is first lost in the coarsest pores, whereas saturation of the material from a dry state means filling of the finest pores first. Figure 23 shows a principle illustration of water in a cement-based material.
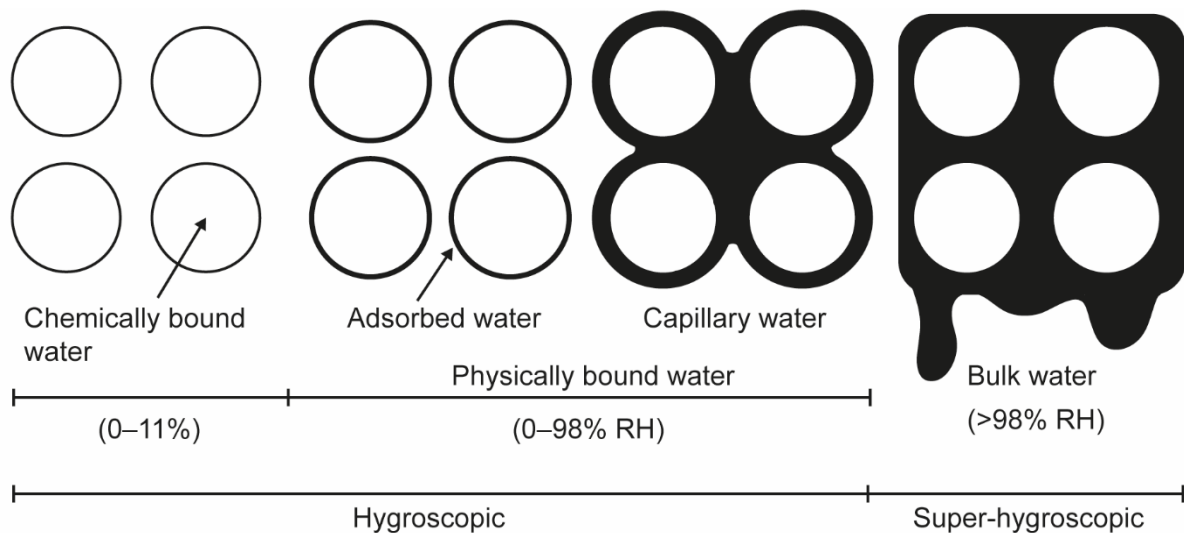
Figure 23
Principle illustration of water in, on and around solid particles in a porous material. Additionally, the approximate RH intervals in which it is lost upon drying are given.

Most of the chemically bound water is only lost if the material is heated to a temperature that causes the hydrates to decompose, as shown in Section 4.2. However, certain hydrates, e.g. part of the C-S-H, AFm, and AFt phases, may be destroyed if the material is dried to a very low RH. According to Feldman and Ramachandran [21, 22], 11% RH is the lower limit below which pore structural alterations occur, not only because some hydrates are destroyed, but because water is irreversibly lost from the interlayer spaces of the C-S-H. Muller et al. [75] suggest that structural alterations already occur as the RH falls below 20–25%, but agree that it is due to water evaporating from the interlayer spaces of the C-S-H. Either way, it may be hard to fully distinguish between the chemically and physically bound water in a cement-based material.

However, there seems to be no agreement as to whether the loss of interlayer water is permanent or reversible. Jennings et al. [62] and Baroghel-Bouny [54] found that water lost from the interlayer spaces could not completely re-enter the structure, even at saturation. Both Jennings et al. [62] and Baroghel-Bouny [54] dried their samples using sealed containers with saturated salt solutions, also known as the desiccator method, in accordance with [79]. Using this method, it may take a very long time to reach equilibrium. As described by Jennings and Thomas [52], a long exposure to low RH may further promote chemical aging of the C-S-H, which could explain the irreversible structural changes reported by [54, 62].

Wu et al. [53] found that if any alterations are apparent at low RH, they are reversed as the sample is re-saturated again. Instead of the desiccator method, they used DVS, which is a much faster method, meaning less time is spent a low RH.
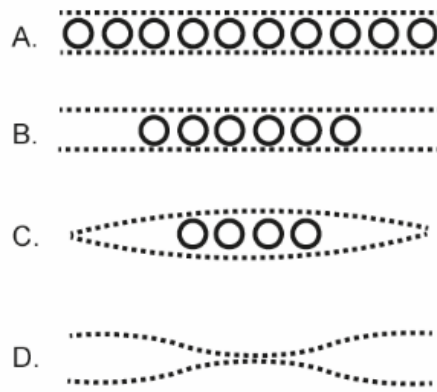
Figure 24
Principle illustration of water exiting the interlayer structure of C-S-H upon drying. Adapted from [80].

Figure 24 A–D illustrates how water exits the interlayer spaces of C-S-H upon drying. Irrespective of whether the structural alterations at low RH are reversible or irreversible, there seems to be consensus that they are caused by a collapse of the C-S-H structure as the interlayer water is lost (Fig. 24, D.). Water exiting the inter-layer spaces below 11% RH may not be able to re-enter until a higher RH, or possibly not at all if bonds form between the collapsed layers.

Water bound physically at low RH (≤ 40%) is known as adsorbed water (Fig. 23), as vapour molecules are adsorbed on the pore surfaces. At higher RH (≥ 40%), capillary condensation occurs, meaning the pores become filled, or partially filled, with condensed liquid or capillary water (Fig. 23). Additionally, bulk water (Fig. 23) may exist in e.g. air voids and micro-cracks close to saturation. The bulk water is not influenced by any surface forces and may thus flow without constraint.

A common tool to calculate how much water is physically bound in a material is to use its sorption isotherm. The sorption isotherm shows moisture content as a function of RH, and may thus be used to predict the moisture content of a material under changing moisture conditions. Isotherms can be measured in absorption or desorption, i.e. going from a dry to a saturated state or vice versa, and the shape of the curve varies depending on the direction. However, the desorption curve is always above the absorption curve. Sorption isotherms of cement-based materials can be found in numerous publications, e.g. [37, 61, 62, 81-84].

The direction-dependent difference between the absorption and desorption isotherms is known as hysteresis. Hysteresis at low RH is often small and can possibly be explained by irreversible changes in the interlayer spaces (e.g. if chemical bonding occur between the surfaces in the dry state Fig. 24, D.) and partial loss of chemically bound water, as discussed earlier. At high RH, capillary condensation is generally described as the main reason for hysteresis, but another possible reason is the so-called ink-bottle effect [85], as illustrated in Fig. 25.
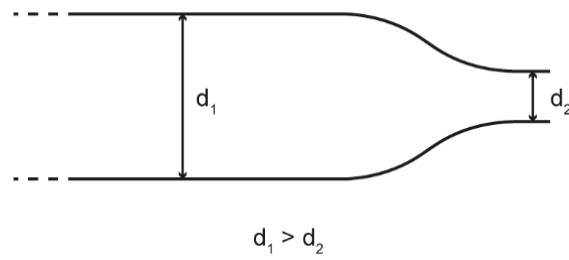
43

Figure 25
Principle illustration of an ink-bottle pore, where d is the diameter.

In ink-bottle pores, the neck and bottle of the pore are emptied and filled at different values of RH, which may give rise to hysteresis. Espinosa and Lutz [61] state that harsh drying and chemical aging of cement-based materials may lead to the formation of ink-bottle pores.

There are mainly two methods used to measure sorption isotherms: the desiccator method and DVS. In this thesis, the latter was used to measure the second desorption isotherms. DVS allows measurements of moisture content in the hygroscopic range (0–98% RH). However, in the present study, 11% RH and is referred to as the dry state in an effort to minimize irreversible structural alterations, thus no moisture content is measured below this level.

To analyse sorption measurements, Jennings's division of pores from the CM-II model [43] is used, but the definitions are slightly modified, both by his own subsequent publication [62], and by the findings of Muller et al. [49, 75]. The resulting interpretation of the porosity, pore sizes and corresponding RH are summarized in Table 4.

Table 4
Division of porosity in the hygroscopic range, with respect to RH and pore sizes.

RH	Porosity	Approximate pore sizes
>90%	Capillary pores	>10 nm
90–80%	Inter-hydrate spaces	8–10 nm
80–50%	Large gel pores	3–8 nm
50–25%	Small gel pores	1–3 nm
25–0%	Intraglobule spaces and interlayer water	<1 nm

Figure 26 shows examples of second desorption isotherms measured by DVS at either 28 days or six months of hydration (some of which are also presented in **Paper III**).
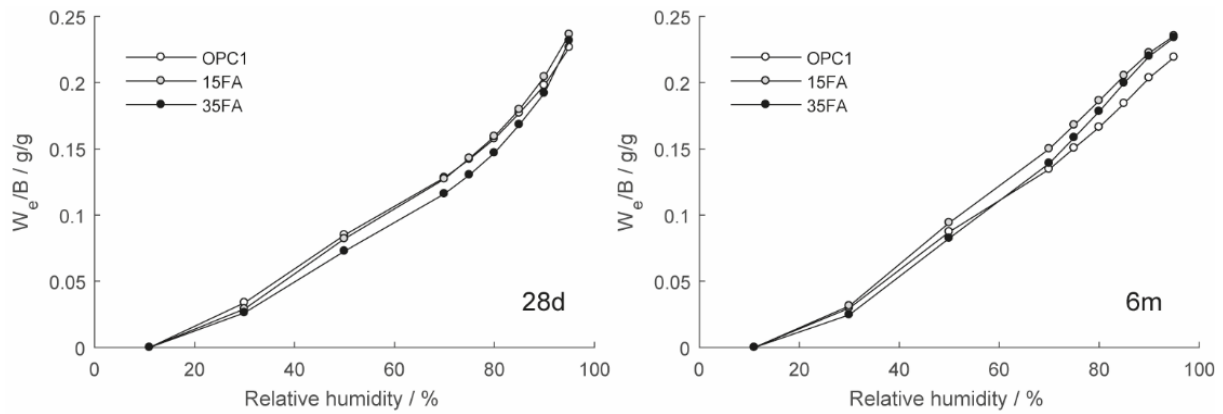
Figure 26
Second desorption isotherms of OPC1, 15FA and 35FA mortars at 28 days (left) and six months (right) of hydration. The samples were hydrated at 20 °C and the isotherms were measured by DVS.

At 28 days, it is evident that less water is physically bound in the 35FA mortar compared to that in 15FA and OPC1. However, a lower fly ash replacement (15FA) does not seem to have as much of an impact on the structural development within the first month, as indicated by the similarities between OPC1 and 15FA isotherms at 28 days. Assuming that the lower half of the curve corresponds to pores intrinsic to the C-S-H gel, it seems only logical that the isotherm of 35FA is lower than the other two, as it was shown in Fig. 18 that the amount of H decreased with the replacement of OPC by 35% fly ash.

Between 28 days and six months, the slopes of the isotherms decrease in the high-RH-range (approximately 80–95%), regardless of the binder composition. This is likely caused by capillary and inter-hydrate pores being refined by the formation of additional hydration products. However, at six months, the order of the isotherms is the opposite of that at 28 days, at least in the upper half of the curve, thus indicating that there are more coarse pores and a larger – hygroscopic – porosity in the fly ash blended mortars. This is in agreement with previous studies, e.g. [6, 69], as was discussed in Section 3.4. Additionally, the TGA results (Fig. 18) show that the total amount of H at six months is notably lower in the 35FA mortar compared to OPC1. This is in agreement with e.g. [16, 69], who both report that α_{FA} is also low (even at modest replacement levels) at this age. Because all three systems (OPC1, 15FA, and 35FA) have the same w/b ratio, and have been cured in sealed moulds, a lower amount of H should result in a higher amount of physically bound water.

Sorption isotherms cannot be used to predict moisture transport and thus the rate of drying, as they do not give any information about how the pores are connected. However, Berodier and Scrivener [69] found that the critical pore entry size is already significantly reduced at a low extent of fly ash reaction, whereas the total porosity is largely unaffected. The critical pore entry size – or threshold diameter – is defined as the smallest channels that are continuous through the cement paste at a given age [86]. This could mean that even minor fly ash reaction significantly reduces the permeability of the material; Winslow et al. [87] reported that the permeability is more sensitive to the threshold diameter (equivalent to the critical pore entry size) than to the total porosity.
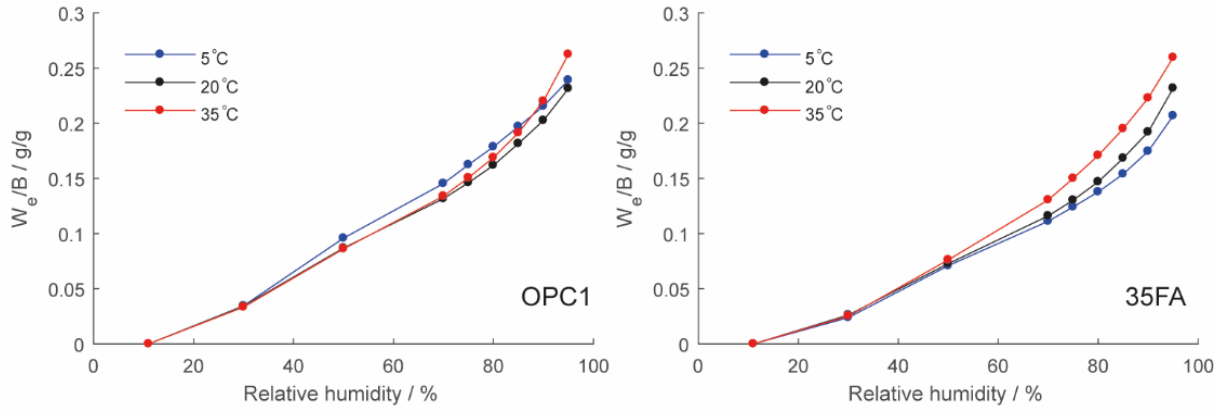
Figure 27
Second desorption isotherms of mortar containing OPC1 and 35FA at 28 days, hydrated at different temperatures during the first 28 days (then at 20 °C), measured by DVS.

Figure 27 shows the second desorption isotherms of OPC1 and 35FA mortars at 28 days, hydrated at different temperatures. In the 35FA mortar, the temperature seems to affect the position of the isotherm, indicating that more moisture is bound at 28 days with increasing temperature. In Fig. 18, there does not seem to be any significant differences between the samples in terms of the amount of H. However, as shown by the SEM images in Fig. 22, there are more coarse pores (of approximately the same size as those referred to here as capillary pores) in the samples hydrated at 35 °C at six months. This is possibly the result of a densification of C-S-H with temperature, causing the number of capillary pores to increase as the C-S-H occupies less space [48].

Interestingly, the curves of OPC1 do not indicate the same temperature dependence as those of 35FA, at least not for the sample hydrated at 5 °C. However, the differences between the other two curves are approximately the same as those found for 35FA. It could be that the 5 °C OPC1 sample is not representative, or that there is an error in the measurement.

It is often the case that sorption isotherms measured by DVS and presented in research papers have not been repeated, which induces uncertainties as to how accurate the results are. A likely reason why they are not repeated is that, although DVS measurements are much quicker than desiccator measurements, it may take weeks to complete a full isotherm (especially for well-hydrated material). Additionally, repeating first desorption isotherms – especially at early age – would require simultaneous measurements and thus multiple DVS instruments.

To counter the uncertainties, some of the isotherms presented in this thesis were repeated, the results of which can be seen in Fig. 28 (also in **Paper III**).
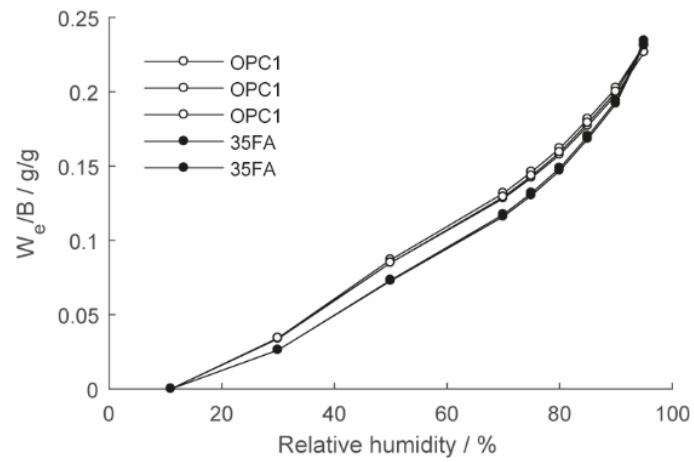
46

Figure 28
Second desorption isotherms of OPC1 and 35FA, hydrated at 20 °C for 28 days, measured by DVS.

As seen in Fig. 28 the second desorption isotherms showed good repeatability. However, these results do not guarantee that all the presented isotherms are accurate, and such certainty cannot be achieved unless each measurement is repeated.

5. Summary of results

General

- The mixing intensity affects the early rate of reaction in cement-based material, and should not be neglected in the experiment design or the following analysis (**Paper I**).

- The binder content in samples of cement-based material can be assessed by dissolving them in hydrochloric acid and then determining the Ca concentration of the acid solution by ICP-OES analysis, as presented in **Paper II.**

- The total amount of chemically bound water – or water bound in specific hydrates – in OPC and fly ash blended OPC mortars can be measured directly by TGA or indirectly by XRD-Rietveld analysis, as presented in Chapter 4 and **Paper III**. The two methods seems to correlate well.

- Second desorption isotherms of OPC and fly ash blended OPC mortars were measured by DVS (see Chapter 4 and **Paper III**).

- Using the mentioned methods, measurements were conducted on samples hydrated at different temperatures (5, 20, 35 °C) during the first 28 days of hydration. Beyond 28 days, all samples were stored at 20 °C.

Replacement level

- The fly ash used in this study does not accelerate the OPC reaction in the first days of hydration, and thus no early filler effect is apparent. This is possibly because the fly ash particles are coarse compared to those of the OPC.

- Replacing part of the OPC by fly ash results in a decrease in the total amount of chemically bound water within the first six months of hydration. A likely reason for this is that fly ash is less hydraulic, and thus that its degree of hydration is lower than that of the OPC. Additionally, previous studies suggest that less water is bound per hydrate in the fly ash reaction, thus making it difficult to assess the degree of hydration from e.g. TGA measurements of fly ash blended samples.

- Partial fly ash replacement seems to enhance the OPC reaction at later age, resulting in a higher degree of OPC hydration at six months according to the XRD-Rietveld results. Possibly, as the fly ash is less hydraulic, it provides additional space for the OPC hydrates to precipitate at ages when they would normally be restrained by a lack of space in a neat OPC system.

- The reactions of C_2S and C_4AF in OPC are significantly accelerated in the fly ash blended mortars. However, only a minor effect was seen for C_3S, which is likely because most of this reaction occurs within the first days of hydration.

- Desorption isotherms show that, after the first month of hydration, less water is physically bound within the hygroscopic RH range in the mortar containing 35% fly ash. At six months of hydration, the order of the isotherms has changed, indicating a higher hygroscopic porosity in the fly ash blended mortars compared to the OPC. This is in agreement with the TGA measurements, showing that less water is chemically bound in the fly ash blended mortars, and thus that more water may be physically bound. However, to fully assess this, the amount of C-S-H gel needs to be determined, as it is the hydrate most responsible for the shape of the sorption isotherms. The amount of C-S-H cannot be accurately derived from e.g. TGA measurements, as the temperature interval in which it decomposes, is similar to that of the AFm and AFt phases.

- With age, the slope of the upper part of the isotherms (approximately 80–95%) decreases, likely because the coarse pores are refined by the formation of additional hydration products.

Curing temperature

- Low curing temperature retards the early reaction, but seems to provide a more homogenous structure that enhances the reaction at later age, resulting in the highest amounts of chemically bound water at six months. The opposite behaviour was seen at high temperature.

- The effect of temperature on the chemically bound water content is less pronounced in the fly ash blended mortars. Together with the XRD-Rietveld results (showing that the degree of hydration in the OPC is increased in the fly ash blended system), this indicates that the fly ash reaction is more sensitive to temperature than that of the OPC.

- The second desorption isotherms of OPC and 35FA mortars hydrated at different temperatures show an increase in porosity with temperature in the upper half of the sorption isotherm. At the same time, the chemically bound water contents are roughly the same. A possible explanation for this is the formation of a denser C-S-H with increasing temperature, as has been reported in previous studies.

- It seems apparent that the early curing temperature has a significant effect on the properties of the material, including at later age.

6. Future research

Chemically bound moisture

- Compare TGA and XRD-Rietveld measurements with heat development from the hydration. By calculating the maximum possible heat development of each binder, measuring the heat development by isothermal calorimetry could yield a triangulation of the degree of hydration. If the methods correlate, it might be possible to calculate the degree of fly ash reaction in blended systems.

Physically bound moisture

- Measure the first desorption isotherms of well-hydrated mortars using DVS, and compare it to the second desorption.

- Compare the sorption isotherms measured by dynamic vapour sorption with isotherms resulting from the desiccator method. Both methods have their advantages and disadvantages, thus using both may resolve some uncertainties as to the accuracy of the observations.

- Study the effect of different w/b ratios on the sorption isotherms of fly ash blended mortars.

Other

- Study the effects of different w/b rations on the hydration kinetics. If fly ash enhances the OPC reaction by providing additional space for its hydrates, as was concluded in this study, then this effect could be delayed, or even eliminated by an increase in the w/b ratio.

- Determine the pore size distributions by e.g. MIP or possibly by solvent exclusion. The latter needs to be further tested for cement-based materials, but has been successfully applied to measure pore sizes in e.g. wood. The measured results could provide information about e.g. the critical pore entry sizes, which may be related to the permeability of the material.

- Conduct moisture transport measurements, e.g. using the cup method. Whereas sorption isotherms provide information about the amount of evaporable moisture, they do not provide information about how the water-filled porosity is connected. Thus, to predict the drying of a concrete structure, moisture transport coefficients are needed. However, studying moisture transport is not an original part of this post-graduate project.

- It would be interesting to perform equivalent measurements to those presented in this thesis on samples containing other supplementary cementitious materials, e.g. slag.

7. References

[1] J. S. Damtoft, J. Lukasik, D. Herfort, D. Sorrentino, and E. M. Gartner, "Sustainable development and climate change initiatives," *Cement and concrete research,* vol. 38, pp. 115-127, 2008.

[2] B. C. Lippiatt and S. Ahmad, "Measuring the life-cycle environmental and economic performance of concrete: the bees approach," presented at the International workshop on sustainable development and concrete technology, Ames, Iowa State University, 2004.

[3] K. L. Scrivener and R. J. Kirkpatrick, "Innovation in use and research on cementitious material," *Cement and Concrete Research,* vol. 38, pp. 128-136, 2// 2008.

[4] K. Scrivener, "Options for the future of cement," *Indian Concrete Journal,* vol. 81, pp. 11-21, 2014.

[5] E. Gartner, "Industrially interesting approaches to "low-CO2" cements," *Cement and Concrete Research,* vol. 34, pp. 1489-1498, 2004/09/01/ 2004.

[6] B. Lothenbach, K. Scrivener, and R. D. Hooton, "Supplementary cementitious materials," *Cement and Concrete Research,* vol. 41, pp. 1244-1256, 12// 2011.

[7] K. L. Scrivener, P. Juilland, and P. J. M. Monteiro, "Advances in understanding hydration of Portland cement," *Cement and Concrete Research,* vol. 78, pp. 38-56, 2015/12/01/ 2015.

[8] G. Baert, S. Hoste, G. De Schutter, and N. De Belie, "Reactivity of fly ash in cement paste studied by means of thermogravimetry and isothermal calorimetry," *Journal of Thermal Analysis and Calorimetry,* vol. 94, pp. 485-492, 2008.

[9] E. Gruyaert, N. Robeyst, and N. De Belie, "Study of the hydration of Portland cement blended with blast-furnace slag by calorimetry and thermogravimetry," *Journal of Thermal Analysis & Calorimetry,* vol. 102, pp. 941-951, 2010.

[10] A. Schöler, B. Lothenbach, F. Winnefeld, M. B. Haha, M. Zajac, and H.-M. Ludwig, "Early hydration of SCM-blended Portland cements: A pore solution and isothermal calorimetry study," *Cement and Concrete Research,* vol. 93, pp. 71-82, 2017/03/01/ 2017.

[11] S. Dittrich, J. Neubauer, and F. Goetz-Neunhoeffer, "The influence of fly ash on the hydration of OPC within the first 44 h—A quantitative in situ XRD and heat flow calorimetry study," *Cement and Concrete Research,* vol. 56, pp. 129-138, 2// 2014.

[12] L. Frølich, L. Wadsö, and P. Sandberg, "Using isothermal calorimetry to predict one day mortar strengths," *Cement and Concrete Research,* vol. 88, pp. 108-113, 2016/10/01/ 2016.

[13] I. Pane and W. Hansen, "Investigation of blended cement hydration by isothermal calorimetry and thermal analysis," *Cement and Concrete Research,* vol. 35, pp. 1155-1164, 2005/06/01/ 2005.

[14] K. De Weerdt, M. B. Haha, G. Le Saout, K. O. Kjellsen, H. Justnes, and B. Lothenbach, "Hydration mechanisms of ternary Portland cements containing limestone powder and fly ash," *Cement and Concrete Research,* vol. 41, pp. 279-291, 3// 2011.

[15] Q. Zeng, K. Li, T. Fen-chong, and P. Dangla, "Determination of cement hydration and pozzolanic reaction extents for fly-ash cement pastes," *Construction and Building Materials,* vol. 27, pp. 560-569, 2// 2012.

[16] K. De Weerdt, M. Ben Haha, G. Le Saout, K. O. Kjellsen, H. Justnes, and B. Lothenbach, "The effect of temperature on the hydration of composite cements containing limestone powder and fly ash," *Materials and Structures,* vol. 45, pp. 1101-1114, 2012.

[17] S. Dittrich, J. Neubauer, and F. Goetz-Neunhoeffer, "The influence of fly ash on the hydration of OPC within the first 44 h-A quantitative in situ XRD and heat flow calorimetry study," *Cement and Concrete Research,* p. 9, 2014.

[18] K. L. Scrivener, T. Füllmann, E. Gallucci, G. Walenta, and E. Bermejo, "Quantitative study of Portland cement hydration by X-ray diffraction/Rietveld analysis and independent methods," *Cement and Concrete Research,* vol. 34, pp. 1541-1547, 9// 2004.

[19] J. I. Escalante-García and J. H. Sharp, "Effect of temperature on the hydration of the main clinker phases in portland cements: part i, neat cements," *Cement and Concrete Research,* vol. 28, pp. 1245-1257, 1998/09/01/ 1998.

[20] J. I. Escalante-García and J. H. Sharp, "Effect of temperature on the hydration of the main clinker phases in portland cements: part ii, blended cements," *Cement and Concrete Research,* vol. 28, pp. 1259-1274, 9// 1998.

[21] R. F. Feldman and V. S. Ramachandran, "Differentiation of interlayer and adsorbed water in hydrated portland cement by thermal analysis," *Cement and Concrete Research,* vol. 1, pp. 607-620, 1971/11/01/ 1971.

[22] R. F. Feldman and V. S. Ramachandran, "A study of the state of water and stoichiometry of bottle-hydrated Ca3SiO5," *Cement and Concrete Research,* vol. 4, pp. 155-166, 1974/03/01/ 1974.

[23] T. C. Powers and T. L. Brownyard, "Studies of the physical properties of hardened Portland cement paste, bulletin 22," *reprinted from Journal of the American Concrete Institute (Proc.),* vol. 43, pp. 101-132, 249-336, 469-504, 549-602, 669-712, 845-880, 933-992, 1948.

[24] X. Hou, R. S. Amais, B. T. Jones, and G. L. Donati, "Inductively Coupled Plasma Optical Emission Spectrometry," in *Encyclopedia of Analytical Chemistry,* ed: John Wiley & Sons, Ltd, 2006.

[25] H. F. W. Taylor, *Cement Chemistry.* London: Thomas Telford, 1997.

[26] I. Odler, "6 - Hydration, Setting and Hardening of Portland Cement A2 - Hewlett, Peter C," in *Lea's Chemistry of Cement and Concrete (Fourth Edition),* ed Oxford: Butterworth-Heinemann, 1998, pp. 241-297.

[27] K. L. Scrivener and A. Nonat, "Hydration of cementitious materials, present and future," *Cement and Concrete Research,* vol. 41, pp. 651-665, 7// 2011.

[28] J. W. Bullard, H. M. Jennings, R. A. Livingston, A. Nonat, G. W. Scherer, J. S. Schweitzer, *et al.,* "Mechanisms of cement hydration," *Cement and Concrete Research,* vol. 41, pp. 1208-1223, 2011/12/01/ 2011.

[29] A. Kumar, S. Bishnoi, and K. L. Scrivener, "Modelling early age hydration kinetics of alite," *Cement and Concrete Research,* vol. 42, pp. 903-918, 2012/07/01/ 2012.

[30] P. Juilland, A. Kumar, E. Gallucci, R. J. Flatt, and K. L. Scrivener, "Effect of mixing on the early hydration of alite and OPC systems," *Cement and Concrete Research,* vol. 42, pp. 1175-1188, 9// 2012.

[31] B. Lothenbach, T. Matschei, G. Möschner, and F. P. Glasser, "Thermodynamic modelling of the effect of temperature on the hydration and porosity of Portland cement," *Cement and Concrete Research,* vol. 38, pp. 1-18, 2008/01/01/ 2008.

[32] J. J. Thomas, H. M. Jennings, and J. J. Chen, "Influence of Nucleation Seeding on the Hydration Mechanisms of Tricalcium Silicate and Cement," *The Journal of Physical Chemistry C,* vol. 113, pp. 4327-4334, 2009/03/19 2009.

[33] L. Nicoleau and A. Nonat, "A new view on the kinetics of tricalcium silicate hydration," *Cement and Concrete Research,* vol. 86, pp. 1-11, 2016/08/01/ 2016.

[34] A. Bazzoni, S. Ma, Q. Wang, X. Shen, M. Cantoni, and K. L. Scrivener, "The Effect of Magnesium and Zinc Ions on the Hydration Kinetics of C3S," *Journal of the American Ceramic Society,* vol. 97, pp. 3684-3693, 2014.

[35] A. Quennoz and K. L. Scrivener, "Interactions between alite and C3A-gypsum hydrations in model cements," *Cement and Concrete Research,* vol. 44, pp. 46-54, 2013/02/01/ 2013.

[36] E. M. J. Berodier, "Impact of the Supplementary Cementitious Materials on the kinetics and microstructural development of cement hydration," Doctoral thesis, Construction Materials, École polytechnique fédérale de Lausanne, Lausanne, Switzerland, 2015.

[37] N. Olsson, L.-O. Nilsson, M. Åhs, and V. Baroghel-Bouny, "Moisture transport and sorption in cement based materials containing slag or silica fume," *Cement and Concrete Research,* vol. 106, pp. 23-32, 4// 2018.

[38] D. Han and R. D. Ferron, "Influence of high mixing intensity on rheology, hydration, and microstructure of fresh state cement paste," *Cement and Concrete Research,* vol. 84, pp. 95-106, 6// 2016.

[39] F. Han, Z. Zhang, J. Liu, and P. Yan, "Hydration kinetics of composite binder containing fly ash at different temperatures," *Journal of Thermal Analysis and Calorimetry,* vol. 124, pp. 1691-1703, 2016.

[40] H. J. H. Brouwers, "The work of Powers and Brownyard revisited: Part 1," *Cement and concrete research,* vol. 34, pp. 1697-1716, 2004.

[41] H. J. H. Brouwers, "The work of Powers and Brownyard revisited: Part 2," *Cement and concrete research,* vol. 35, pp. 1922-1936, 2005.

[42] A. Nonat, "The structure and stoichiometry of C-S-H," *Cement and Concrete Research,* vol. 34, pp. 1521-1528, 9// 2004.

[43] H. M. Jennings, "Refinements to colloid model of C-S-H in cement: CM-II," *Cement and Concrete Research,* vol. 38, pp. 275-289, 3// 2008.

[44] H. M. Jennings, "A model for the microstructure of calcium silicate hydrate in cement paste," *Cement and Concrete Research,* vol. 30, pp. 101-116, 2000/01/01/ 2000.

[45] I. G. Richardson, "The calcium silicate hydrates," *Cement and Concrete Research,* vol. 38, pp. 137-158, 2008/02/01/ 2008.

[46] P. D. Tennis and H. M. Jennings, "A model for two types of calcium silicate hydrate in the microstructure of Portland cement pastes," *Cement and Concrete Research,* vol. 30, pp. 855-863, 6// 2000.

[47] A. Bazzoni, "Study of early hydration mechanisms of cement by means of electron microscopy," EPFL.

[48] E. Gallucci, X. Zhang, and K. L. Scrivener, "Effect of temperature on the microstructure of calcium silicate hydrate (C-S-H)," *Cement and Concrete Research,* vol. 53, pp. 185-195, 2013/11/01/ 2013.

[49] A. C. A. Muller, K. L. Scrivener, A. M. Gajewicz, and P. J. McDonald, "Densification of C–S–H Measured by 1H NMR Relaxometry," *The Journal of Physical Chemistry C,* vol. 117, pp. 403-412, 2013/01/10 2013.

[50] R. F. Feldman and P. J. Sereda, "A new model for hydrated Portland cement and its practical implications," *Engineering Journal (Montreal),* vol. 53, pp. 53-69, 1970.

[51] J. J. Thomas and H. M. Jennings, "Effect of Heat Treatment on the Pore Structure and Drying Shrinkage Behavior of Hydrated Cement Paste," *Journal of the American Ceramic Society,* vol. 85, pp. 2293-2298, 2002.

[52] J. J. Thomas and H. M. Jennings, "A colloidal interpretation of chemical aging of the C-S-H gel and its effects on the properties of cement paste," *Cement and Concrete Research,* vol. 36, pp. 30-38, 2006/01/01/ 2006.

[53] M. Wu, B. Johannesson, and M. Geiker, "A study of the water vapor sorption isotherms of hardened cement pastes: Possible pore structure changes at low relative humidity and the impact of temperature on isotherms," *Cement and Concrete Research,* vol. 56, pp. 97-105, 2014/02/01/ 2014.

[54] V. Baroghel-Bouny, "Water vapour sorption experiments on hardened cementitious materials: Part I: Essential tool for analysis of hygral behaviour and its relation to pore structure," *Cement and Concrete Research,* vol. 37, pp. 414-437, 2007/03/01/ 2007.

[55] Y. Maltais and J. Marchand, "Influence of curing temperature on cement hydration and mechanical strength development of fly ash mortars," *Cement and Concrete Research,* vol. 27, pp. 1009-1020, 7// 1997.

[56] K. O. Kjellsen, R. J. Detwiler, and O. E. Gjørv, "Development of microstructures in plain cement pastes hydrated at different temperatures," *Cement and Concrete Research,* vol. 21, pp. 179-189, 1991/01/01/ 1991.

[57] F. Deschner, B. Lothenbach, F. Winnefeld, and J. Neubauer, "Effect of temperature on the hydration of Portland cement blended with siliceous fly ash," *Cement and Concrete Research,* vol. 52, pp. 169-181, 2013/10/01/ 2013.

[58] S. Bishnoi and K. L. Scrivener, "Studying nucleation and growth kinetics of alite hydration using μic," *Cement and Concrete Research,* vol. 39, pp. 849-860, 2009/10/01/ 2009.

[59] J. I. Escalante-Garcia and J. H. Sharp, "The chemical composition and microstructure of hydration products in blended cements," *Cement and Concrete Composites,* vol. 26, pp. 967-976, 2004/11/01/ 2004.

[60] J. I. Escalante-García and J. H. Sharp, "The microstructure and mechanical properties of blended cements hydrated at various temperatures," *Cement and Concrete Research,* vol. 31, pp. 695-702, 5// 2001.

[61] R. M. Espinosa and L. Franke, "Influence of the age and drying process on pore structure and sorption isotherms of hardened cement paste," *Cement and Concrete Research,* vol. 36, pp. 1969-1984, 2006/10/01/ 2006.

[62] H. M. Jennings, A. Kumar, and G. Sant, "Quantitative discrimination of the nano-pore-structure of cement paste during drying: New insights from water sorption isotherms," *Cement and Concrete Research,* vol. 76, pp. 27-36, 10// 2015.

[63] C. Gallé, "Effect of drying on cement-based materials pore structure as identified by mercury intrusion porosimetry: A comparative study between oven-, vacuum-, and freeze-drying," *Cement and Concrete Research,* vol. 31, pp. 1467-1477, 2001/10/01/ 2001.

[64] D. Snoeck, L. F. Velasco, A. Mignon, S. Van Vlierberghe, P. Dubruel, P. Lodewyckx, *et al.,* "The influence of different drying techniques on the water sorption properties of cement-based materials," *Cement and Concrete Research,* vol. 64, pp. 54-62, 2014/10/01/ 2014.

[65] E. Berodier and K. Scrivener, "Understanding the Filler Effect on the Nucleation and Growth of C-S-H," *Journal of the American Ceramic Society,* vol. 97, pp. 3764-3773, 2014.

[66] W. A. Gutteridge and J. A. Dalziel, "Filler cement: The effect of the secondary component on the hydration of Portland cement: Part I. A fine non-hydraulic filler," *Cement and Concrete Research,* vol. 20, pp. 778-782, 1990/09/01/ 1990.

[67] *NATIONAL READY MIXED CONCRETE ASSOCIATION (NRMCA) webpage. Available from: http//nrmca.org/.*

[68] R. Taylor, I. G. Richardson, and R. M. D. Brydson, "Composition and microstructure of 20-year-old ordinary Portland cement–ground granulated blast-furnace slag blends containing 0 to 100% slag," *Cement and Concrete Research,* vol. 40, pp. 971-983, 2010/07/01/ 2010.

[69] E. Berodier and K. Scrivener, "Evolution of pore structure in blended systems," *Cement and Concrete Research,* vol. 73, pp. 25-35, 2015/07/01/ 2015.

[70] R. E. Davis, R. W. Carlson, J. W. H. Kelly, and H. E. Davis, "Properties Of Cements And Concretes Containing Fly Ash," *Journal of the American Concrete Institute,* vol. 33, pp. 577-611, 5/1/1937 1937.

[71] R. C. Joshi and R. P. Lohita, *Fly Ash in Concrete: Production, Properties and Uses*: Taylor & Francis, 1997.

[72] A. M. Neville, *Properties of Concrete*: Pearson, 2011.

[73] G. Fagerlund, "10 - Struktur och strukturutveckling," in *Betonghandboken,* ed Stockholm: AB Svensk Byggtjänst, 2017.

[74] J. S. Dolado, M. Griebel, J. Hamaekers, and F. Heber, "The nano-branched structure of cementitious calcium-silicate-hydrate gel," *Journal of Materials Chemistry,* vol. 21, pp. 4445-4449, 2011.

[75] A. C. A. Muller, K. L. Scrivener, A. M. Gajewicz, and P. J. McDonald, "Use of bench-top NMR to measure the density, composition and desorption isotherm of C–S–H in cement paste," *Microporous and Mesoporous Materials,* vol. 178, pp. 99-103, 2013/09/15/ 2013.

[76] K. L. Scrivener and K. M. Nemati, "The percolation of pore space in the cement paste/aggregate interfacial zone of concrete," *Cement and Concrete Research,* vol. 26, pp. 35-40, 1996/01/01/ 1996.

[77] K. L. Scrivener, A. K. Crumbie, and P. Laugesen, "The Interfacial Transition Zone (ITZ) Between Cement Paste and Aggregate in Concrete," *Interface Science,* vol. 12, pp. 411-421, October 01 2004.

[78] K. De Weerdt, M. Ben Haha, G. Le Saout, K. O. Kjellsen, H. Justnes, and B. Lothenbach, "Hydration mechanisms of ternary Portland cements containing limestone powder and fly ash," *Cement and concrete research,* vol. 41, pp. 279-291, 2011.

[79] L. Greenspan, *Humidity Fixed Points of Binary Saturated Aqueous Solutions* vol. 81A, 1977.

[80] R. F. Feldman and P. J. Sereda, "A model for hydrated Portland cement paste as deduced from sorption-length change and mechanical properties," *Matériaux et Construction,* vol. 1, pp. 509-520, November 01 1968.

[81] E. Helsing Atlassi, "Influence of Silica Fume on the Pore Structure of Mortar when Measured by Water Vapour Sorption Isotherms," in *The Modelling of Microstructure and its Potential for Studying Transport Properties and Durability,* H. Jennings, J. Kropp, and K. Scrivener, Eds., ed Dordrecht: Springer Netherlands, 1996, pp. 257-270.

[82] M. Saeidpour and L. Wadsö, "Moisture equilibrium of cement based materials containing slag or silica fume and exposed to repeated sorption cycles," *Cement and Concrete Research,* vol. 69, pp. 88-95, 2015/03/01/ 2015.

[83] M. S. Åhs, "Sorption scanning curves for hardened cementitious materials," *Construction and Building Materials,* vol. 22, pp. 2228-2234, 2008/11/01/ 2008.

[84] X. Aimin, *Structure of hardened cement fly ash systems and their related properties:* Division of Building Materials, Chalmers University of Technology, 1992.

[85] R. M. Espinosa and L. Franke, "Inkbottle Pore-Method: Prediction of hygroscopic water content in hardened cement paste at variable climatic conditions," *Cement and Concrete Research,* vol. 36, pp. 1954-1968, 2006/10/01/ 2006.

[86] W. R. Wise, "A new insight on pore structure and permeability," *Water Resources Research,* vol. 28, pp. 189-198, 1992.

[87] D. N. Winslow, M. D. Cohen, D. P. Bentz, K. A. Snyder, and E. J. Garboczi, "Percolation and pore structure in mortars and concrete," *Cement and Concrete Research,* vol. 24, pp. 25-37, 1994/01/01/ 1994.